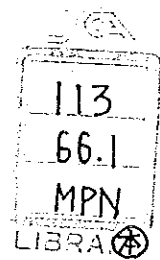


REPORT ON THE COLLABORATIVE
MINERAL EXPLORATION OF THE
SABAH AREA, MALAYSIA

PHASE I

OCTOBER, 1986







REPORT ON THE COLLABORATIVE
MINERAL EXPLORATION OF THE
SABAH AREA, MALAYSIA

PHASE I
OCTOBER, 1986

MJ
MI
AC
JA

MALAYSIA

**REPORT ON THE COLLABORATIVE
MINERAL EXPLORATION OF
SABAH AREA**

PHASE I

OCTOBER, 1986

**JAPAN INTERNATIONAL COOPERATION AGENCY
METAL MINING AGENCY OF JAPAN**



113
661
MPN
LIBRARY
751-00

**M P N
CR (3)
86-132**

MALAYSIA

**REPORT ON THE COLLABORATIVE
MINERAL EXPLORATION OF
SABAH AREA**

PHASE I

 **LIBRARY**



1031316E1J

OCTOBER, 1986

**JAPAN INTERNATIONAL COOPERATION AGENCY
METAL MINING AGENCY OF JAPAN**

国際協力事業団		
受入 月日	87.1.12	113
登録 No.	15730	66.1 MPN

PREFACE

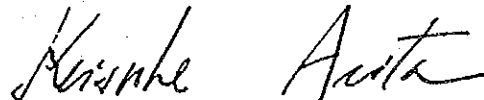
The Government of Japan, in response to a request from the Government of Malaysia, agreed to conduct a collaborative mineral exploration project with the Geological Survey of Malaysia in the Ranau area, Sabah, Malaysia. The project is a Fifth Malaysia Plan project proposed by the Geological Survey of Malaysia to be implemented by the department with foreign bilateral assistance. The Government of Japan entrusted the implementation of its assistance to the Japan International Cooperation Agency and the Metal Mining Agency of Japan. This project is designed to be carried out in three phases spaced over three years commencing at the beginning of August, 1985.

Phase I of the project consisting mainly of geological, geochemical survey, geophysical survey and drilling was accomplished jointly by a Japanese team and staff of the Geological Survey of Malaysia, Sabah, in 1986.

This report summarizes the results of the afore-mentioned undertaking and also forms a part of the final consolidated report which will be submitted to the Government of Malaysia after completion of the project.

We wish to express our appreciation for the close and mutually beneficial cooperation that exists between the implementing agencies of both the Japanese and Malaysian Governments and to the various organizations, particularly the Japanese Embassy in Malaysia and government departments in Kota Kinabalu, Sabah, which have rendered assistance in one way or another during the course of the project.

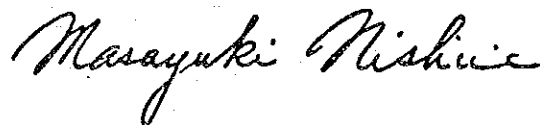
August, 1986



Keisuke Arita

President

Japan International Cooperation Agency



Masayuki Nishiie

President

Metal Mining Agency of Japan

Yin Ee Heng

Director-General

Geological Survey of Malaysia

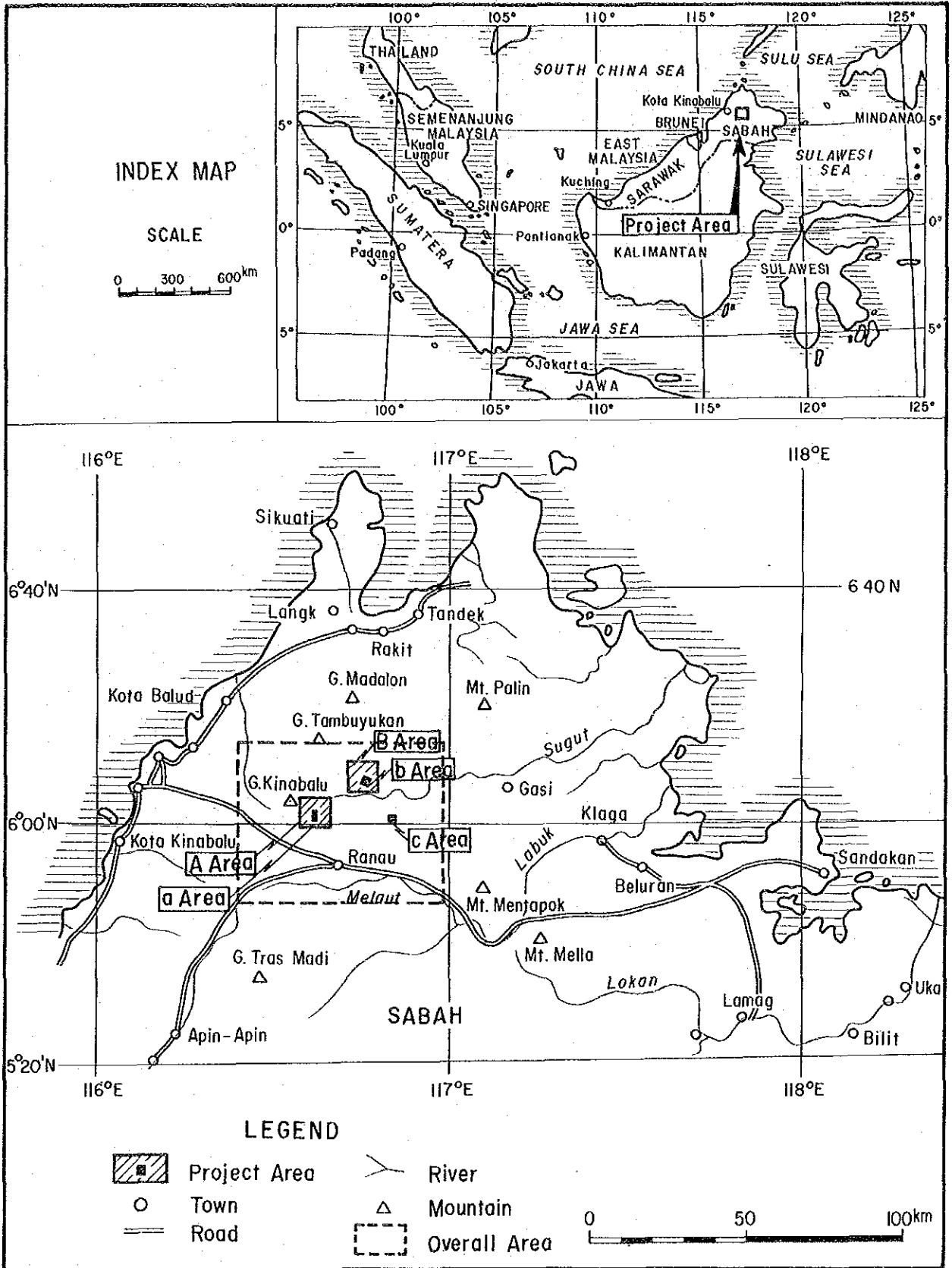


Fig. 1 Location Map of Survey Area

Contents

PREFACE	
LOCATION MAP	
CONTENTS	
ABSTRACT	

PART 1 INTRODUCTION

Chapter 1	Outline of Survey	1
1-1	Background and Purpose of Survey	1
1-2	Contents of Survey	1
1-3	Organization of Mission	3
Chapter 2	Geography of Survey Area	7
2-1	Location and Accessibility	7
2-2	Topography	7
2-3	Climate and Vegetation	9
Chapter 3	General Geology and Previous Surveys	11
3-1	Geology of SABAH Region	11
3-2	Geological Setting of Project Area	13
3-3	Previous Surveys	21

PART II A, a (BAMBANGAN) AREA

Chapter 1	Geology and Mineralization	25
1-1	Geology	25
1-2	Mineralization	25
Chapter 2	Geophysical Survey	29
2-1	CSAMT Survey	29
2-1-1	Objectives and Method of Survey	29
2-1-2	Data Analysis	34
2-1-3	Result of Survey	36
2-1-4	Discussion	58
2-2	IP and SIP Surveys	61

2-2-1	Objectives and Method of Survey	61
2-2-2	Data Analysis	66
2-2-3	Result of Survey	80
2-2-4	Discussion	104
Chapter 3	Drilling	109
3-1	Process of Drilling and Equipment	109
3-2	Result of Drilling	141
Chapter 4	Overall Discussion	171

PART III B, b (MANKADAU) AREA

Chapter 1	Geology and Mineralization	173
1-1	Geology	173
1-2	Mineralization	184
Chapter 2	Geochemical Survey (Soil)	197
2-1	Field Procedure	197
2-2	Laboratory Procedure	197
2-3	Data Analysis	197
2-4	Result of Survey	207
2-5	Discussion	210
Chapter 3	Geophysical Survey (CSAMT Method)	215
3-1	Content of Survey	215
3-2	Result of Survey	215
3-3	Discussion	234
Chapter 4	Overall Discussion	237

PART IV c (PALIU) AREA

Chapter 1	Geology and Mineralization	239
1-1	Geology	239
1-2	Mineralization	250
Chapter 2	Geochemical Survey	263
2-1	Soil Survey	263

2-1-1	Field Procedure and Data Analysis	263
2-1-2	Result of Survey	263
2-1-3	Discussion	277
2-2	Drainage Survey	281
2-2-1	Field Procedure	281
2-2-2	Laboratory Procedure	281
2-2-3	Data Analysis	281
2-2-4	Result of Survey	281
2-2-5	Discussion	288
Chapter 3	Overall Discussion	291

PART V CONCLUSION AND RECOMMENDATION

1.	Conclusion	293
2.	Recommendation for Phase II Survey	294

REFERENCES

LIST OF ILLUSTRATIONS

Fig. 1	Location Map of Survey Area
Fig. 2	Location Map of Phase I Area
Fig. 3	Generalized Geological Map of SABAH
Fig. 4	Geological Map of West SABAH
Fig. 5	Geological Map of KINABALU Area
Fig. 6	Generalized Stratigraphic Section of Survey Area
Fig. 7	Geological Map of "A" Area
Fig. 8	CSAMT 3-D Display over a Massive Sulfide Orebody
Fig. 9	Logistics of CSAMT Survey
Fig. 10	Apparent Resistivity Plan Map in "A" Area (2048Hz)
Fig. 11	Apparent Resistivity Plan Map in "A" Area (1024Hz)
Fig. 12	Apparent Resistivity Plan Map in "A" Area (512Hz)
Fig. 13	Apparent Resistivity Plan Map in "A" Area (256Hz)
Fig. 14	Apparent Resistivity Plan Map in "A" Area (128Hz)
Fig. 15	Apparent Resistivity Section in "A" Area (Section A)
Fig. 16	Apparent Resistivity Section in "A" Area (Section B)
Fig. 17	Apparent Resistivity Section in "A" Area (Section C)
Fig. 18	Apparent Resistivity Section in "A" Area (Section D)
Fig. 19	Resistivity Structural Map in "A" Area (50m)
Fig. 20	Resistivity Structural Map in "A" Area (150m)
Fig. 21	Resistivity Structural Map in "A" Area (200m)
Fig. 22	Resistivity Section in "A" Area (Section A)
Fig. 23	Resistivity Section in "A" Area (Section B)
Fig. 24	Resistivity Section in "A" Area (Section C)
Fig. 25	Resistivity Section in "A" Area (Section D)
Fig. 26	CSAMT Interpretation Map in "A" Area
Fig. 27	Location Map of SIP and IP Survey Lines in "A" Area
Fig. 28	Potential Electrode Configuration
Fig. 29	Diagram of SIP Survey System
Fig. 30	Physical Property of Measuring System
Fig. 31-1~4	Spectrum for Rock Samples
Fig. 32-1~5	2-D Model Calculation

Fig. 33-1~3	Apparent Resistivity Pseudosection
Fig. 34-1~3	PFE Pseudosection
Fig. 35-1~2	Phase Pseudosection
Fig. 36-1~2	3-pt Decoupled Phase Pseudosection
Fig. 37-1~3	Apparent Resistivity Plan Map
Fig. 38-1~3	PFE Plan Map
Fig. 39	Phase Spectrum Diagram (Line-B, D, SE, F, H)
Fig. 40	Magnitude Spectrum Diagram (Line-B, D, SE, F, H)
Fig. 41	Cole-Cole Diagram (Line-B, D, SE, F, H)
Fig. 42	Geophysical Interpretation Map of "A" Area
Fig. 43	Location Map of Drill Hole
Fig. 44-1~10	Progress Record of Drilling (MJM-1 to MJM-10)
Fig. 45-1~10	Columnar Section of Drill Hole (MJM-1 to MJM-10)
Fig. 46	Sketch of Drill Core
Fig. 47-1~10	Geological Section of Drill Hole (MJM-1 to MJM-10)
Fig. 48	Schematic Geological Section in "a" Area
Fig. 49	Normative Q-Kf-Pl Diagram of Intrusive Rocks in the Drill Holes
Fig. 50	Alteration Pattern of Serpentinized Peridotite
Fig. 51	Characteristics of Pinosuk Gravels at MJM-6 and -9 Holes
Fig. 52	Geological Map of "b" Area
Fig. 53	Generalized Stratigraphic Section of "b" Area
Fig. 54	Na ₂ O + K ₂ O - SiO ₂ Diagram of Basalt
Fig. 55	SiO ₂ - total Fe/MgO Diagram of Basalt
Fig. 56	Structural Map of "b" Area
Fig. 57	Rose Diagram of Structural Elements in "b" Area
Fig. 58	Distribution of Alteration Zone in "b" Area
Fig. 59	Sketch Showing Copper Boulder
Fig. 60	Sketch Showing Chromite Boulder
Fig. 61	Location Map of Soil Samples in "b" Area
Fig. 62	Histogram for Soil Samples in "b" Area
Fig. 63	Cumulative Frequency Curve for Soil Samples in "b" Area
Fig. 64	Geochemical Interpretation Map of "b" Area
Fig. 65	Apparent Resistivity Plan Map in "B" Area (2048Hz)
Fig. 66	Apparent Resistivity Plan Map in "B" Area (1024Hz)

Fig. 67	Apparent Resistivity Plan Map in "B" Area (512Hz)
Fig. 68	Apparent Resistivity Plan Map in "B" Area (256Hz)
Fig. 69	Apparent Resistivity Plan Map in "B" Area (128Hz)
Fig. 70	Apparent Resistivity Section in "B" Area (Section E)
Fig. 71	Apparent Resistivity Section in "B" Area (Section F)
Fig. 72	Apparent Resistivity Section in "B" Area (Section G)
Fig. 73	Resistivity Structural Map in "B" Area (50m)
Fig. 74	Resistivity Structural Map in "B" Area (150m)
Fig. 75	Resistivity Structural Map in "B" Area (200m)
Fig. 76	Resistivity Section in "B" Area (Section E)
Fig. 77	Resistivity Section in "B" Area (Section F)
Fig. 78	Resistivity Section in "B" Area (Section G)
Fig. 79	CSAMT Interpretation Map in "B" Area
Fig. 80	Geological Map of "c" Area
Fig. 81	Generalized Stratigraphic Section of "c" Area
Fig. 82	Geological Columnar Sections of "c" Area
Fig. 83	Normative Q-Kf-Pl Diagram of Intrusive Rocks in "c" Area
Fig. 84	Structural Map of "c" Area
Fig. 85	Rose Diagram of Structural Elements in "c" Area
Fig. 86	Distribution of Alteration Zone in "c" Area
Fig. 87	Sketch Showing Quartz Vein
Fig. 88	Sketch Showing Mineralization by Intrusive Rock
Fig. 89	Location Map of Soil Samples in "c" Area
Fig. 90	Histogram for Soil Samples in "c" Area
Fig. 91	Cumulative Frequency Curve for Soil Samples in "c" Area
Fig. 92	Geochemical Interpretation Map of "c" Area
Fig. 93	Location Map of Stream Sediment Samples in "c" Area
Fig. 94	Histogram for Stream Sediment Samples in "c" Area
Fig. 95	Cumulative Frequency Curve for Stream Sediment Samples in "c" Area
Fig. 96	Score-Sum Map of Stream Sediment Samples in "c" Area

LIST OF TABLES

Table 1	Outline of Field Survey in Phase I
Table 2	Records of Monthly Rainfall
Table 3	Specifications and Survey Amount for CSAMT Survey in "A" Area
Table 4	Specifications and Survey Amount for IP, SIP Survey in "A" Area
Table 5	Physical Property
Table 6--1~2	Specifications of Drilling Machine
Table 7--1~3	Drilling Meterage by Diamond Bit
Table 8	Details of Consumed Materials
Table 9--1~2	Timetable of Drilling Work
Table 10--1~11	Summary Record of Drilling Work
Table 11	Characteristics of CSAMT Anomalous zones
Table 12	Chemical Composition of Ultrabasic Rock
Table 13	Chemical Composition and CIPW Norm of Basalt
Table 14	Chemical Composition of Copper Boulder
Table 15	Chemical Composition of Chromite Boulder
Table 16	Statistic Values for Soil Samples in "b" Area
Table 17	Specifications and Survey Amount for CSAMT Survey in "b" Area
Table 18	Chemical Composition and CIPW Norm of Intrusive Rock
Table 19	Statistic Values for Soil Samples in "c" Area
Table 20	Result of Factor Analysis
Table 21	Statistic Values for Stream Sediment Samples in "c" Area

LIST OF APPENDICES

A-1	Microphotograph of Thin Sections
A-2	Microphotograph of Polished Sections
A-3	Result of Thin Section Examination
A-4	Result of Polished Section Examination
A-5	Result of X-ray Diffractive Analysis
A-6	Result of Chemical Analysis of Ores
A-7	Result of Chemical Analysis of Whole Rocks
A-8	Detection Limits and Analytical Methods
A-9	Result of Chemical Analysis of Soil Samples
A-10	Result of Chemical Analysis of Stream Sediment Samples
A-11	Assay Result of Drill Core
A-12	SIP Phase Pseudosections
A-13	Records of Drilling Works

LIST OF MAPS

Map-1	Geological Map of KINABALU Area
Map-2	Location Map of Survey Area and Current Dipole
Map-3	Location Map of Stations and Sections ("A" Area)
Map-4	Apparent Resistivity Plan Map [2048 Hz] ("A" Area)
Map-5	Apparent Resistivity Plan Map [1024 Hz] ("A" Area)
Map-6	Apparent Resistivity Plan Map [512 Hz] ("A" Area)
Map-7	Apparent Resistivity Plan Map [256 Hz] ("A" Area)
Map-8	Apparent Resistivity Plan Map [128 Hz] ("A" Area)
Map-9	Apparent Resistivity Plan Map [64 Hz] ("A" Area)
Map-10	Apparent Resistivity Plan map [32 Hz] ("A" Area)
Map-11	Apparent Resistivity Plan map [16 Hz] ("A" Area)
Map-12	Apparent Resistivity Plan Map [8 Hz] ("A" Area)
Map-13	Apparent Resistivity Plan Map [4 Hz] ("A" Area)
Map-14	Resistivity Structure Map [50 m] ("A" Area)
Map-15	Resistivity Structure Map [150 m] ("A" Area)
Map-16	Resistivity Structure Map [200 m] ("A" Area)
Map-17	CSAMT Interpretation Map ("A" Area)
Map-18	Location Map of Survey Area and SIP, IP Line ("A" Area)
Map-19	Apparent Resistivity Section Map [Line-A,B,C] ("A" Area)
Map-20	Apparent Resistivity Section Map [Line-D,E,F] ("A" Area)
Map-21	Apparent Resistivity Section Map [Line-G,H,SE] ("A" Area)
Map-22	Frequency Effect Section Map [Line-A,B,C] ("A" Area)
Map-23	Frequency Effect Section Map [Line-D,E,F] ("A" Area)
Map-24	Frequency Effect Section Map [Line-G,H,SE] ("A" Area)
Map-25	Apparent Resistivity Map [N-Spread(1)] ("A" Area)
Map-26	Apparent Resistivity Map [N-Spread(3)] ("A" Area)
Map-27	Apparent Resistivity Map [N-Spread(5)] ("A" Area)
Map-28	Frequency Effect Map [N-Spread(1)] ("A" Area)
Map-29	Frequency Effect Map [N-Spread(3)] ("A" Area)
Map-30	Frequency Effect Map [N-Spread(5)] ("A" Area)
Map-31	Geophysical Interpretation Map ("A" Area)
Map-32	Drilling Core Record (1/200)

Map-33	Geological Map ("b" Area)
Map-34	Geological Profile ("b" Area)
Map-35	Distribution of Alteration Zone ("b" Area)
Map-36	Location Map of Tested Samples ("b" Area)
Map-37	Location Map of Soil Samples ("b" Area)
Map-38	Distribution of Cu in Soil Samples ("b" Area)
Map-39	Distribution of Pb in Soil Samples ("b" Area)
Map-40	Distribution of Zn in Soil Samples ("b" Area)
Map-41	Score-Sum Map of Soil Samples ("b" Area)
Map-42	Geochemical Interpretation Map ("b" Area)
Map-43	Location Map of Stations and Sections ("B" Area)
Map-44	Apparent Resistivity Plan Map [2048 Hz] ("B" Area)
Map-45	Apparent Resistivity Plan Map [1024 Hz] ("B" Area)
Map-46	Apparent Resistivity Plan Map [512 Hz] ("B" Area)
Map-47	Apparent Resistivity Plan Map [256 Hz] ("B" Area)
Map-48	Apparent Resistivity Plan Map [128 Hz] ("B" Area)
Map-49	Apparent Resistivity Plan Map [64 Hz] ("B" Area)
Map-50	Apparent Resistivity Plan Map [32 Hz] ("B" Area)
Map-51	Apparent Resistivity Plan Map [16 Hz] ("B" Area)
Map-52	Apparent Resistivity Plan Map [8 Hz] ("B" Area)
Map-53	Apparent Resistivity Plan Map [4 Hz] ("B" Area)
Map-54	Resistivity Structural Map [50 m] ("B" Area)
Map-55	Resistivity Structural Map [150 m] ("B" Area)
Map-56	Resistivity Structural Map [200 m] ("B" Area)
Map-57	CSAMT Interpretation Map ("B" Area)
Map-58	Geological Map ("c" Area)
Map-59	Geological Profile ("c" Area)
Map-60	Geological Columnar Section ("c" Area)
Map-61	Distribution of Alteration Zone ("c" Area)
Map-62	Location Map of Tested Samples ("c" Area)
Map-63	Location Map of Soil Samples ("c" Area)
Map-64	Distribution of Cu in Soil Samples ("c" Area)
Map-65	Distribution of Pb in Soil Samples ("c" Area)
Map-66	Distribution of Zn in Soil Samples ("c" Area)

Map-67	Distribution of Mo in Soil Samples ("c" Area)
Map-68	Distribution of Au in Soil Samples ("c" Area)
Map-69	Score-Sum Map of Soil Samples ("c" Area)
Map-70	Distribution of Factor Score for Whole Rock in Soil Samples ("c" Area)
Map-71	Distribution of Factor Score for Intrusive Rock in Soil Samples ("c" Area)
Map-72	Distribution of Factor Score for Sedimentary Rock in Soil Samples ("c" Area)
Map-73	Geochemical Interpretation Map ("c" Area)
Map-74	Location Map of Stream Sediment Samples ("c" Area)
Map-75	Distribution of Cu in Stream Sediment Samples ("c" Area)
Map-76	Distribution of Pb in Stream Sediment Samples ("c" Area)
Map-77	Distribution of Zn in Stream Sediment Samples ("c" Area)
Map-78	Score-Sum Map of Stream Sediment Samples ("c" Area)

ABSTRACT

In the Kinabalu Mountain area, Sabah, Malaysia, the geosynclinal sediments from late Cretaceous to early Miocene are widely distributed, and structurally intruded by peridotite which was accompanied by strong faulting and uplifting in the latest Miocene. At the end of Miocene intermediate to acidic plutonic rocks intruded in the later orogenic stage and followed by hypoabyssal volcanic activities.

The Mamut ore deposit is of a porphyry copper type accompanied by adamellite porphyry intrusion, having of its scale of 800 m in a N-S direction and 300 m in a E-W direction.

In Phase I of the collaborative mineral exploration, geological, geochemical and geophysical surveys (CSAMT, IP and SIP methods) and drillings were carried out in the following three areas which seem to have high potentials for copper mineralization from the existing data.

The survey results can be summarized as follows;

(1) Banbangan area

The area is located in the west side of Mamut deposit, overlain by thick Pinosuk Gravels of Quaternary period.

Along the Bambangan Creek there are some zone of copper mineralization accompanied by adamellite porphyry, where geochemical copper anomalies were detected in stream sediment and soil.

The CSAMT survey was carried out in the area of 100 km² (A-area) to delineate the resistivity structure underlying Pinosuk Gravels and detected three anomalous resistivity zones with the figure of lower than 50 ohm-m.

Other electric surveys (IP and SIP methods) were followed in the most promising zones among three to confirm the alteration and sulphide mineralization. As a result, an IP anomalous zone extending to N-S direction was detected on the west bank of Bambangan Creek as may be caused by sulphide mineralization.

The diamond drilling of 10 holes with a total length of 3,456.20 m, was carried out near the Bambangan Creek to test the lower mineralized horizons and the IP anomalous zones.

As a result, the followings were clarified.

(a) In the known mineralized zone, the adamellite porphyry dykes become thinner and the copper mineralizations weaken toward depth.

(b) In the IP anomalous zone, the drilling intersected the copper mineralized zone in adamellite porphyry. The length of mineralization in the hole is more than 83.90 m with the portions of better grade.

(c) The Pinosuk Gravels is getting thicker toward east from the Bambang Creek, showing more than 270 m thick.

(2) Mankadau area

The area is widely occupied by the peridotite. The floats of high grade massive copper sulphide ore distribute in the Lingangaa Creek, a branch of the Mankadau River.

For the purpose of investigation of its source, the geochemical survey by soil and the CSAMT survey were carried out in the areas of 4 km² (b area) and 100 km² (B area), respectively.

The values of Cu, Pb and Zn contents were generally low and no geochemical anomalies were detected.

The CSAMT survey disclosed high resistivity zones corresponding to the shape of peridotite and presumed that low resistivity zones near the peridotite may indicate strong argillization along faults.

(3) Paliu area

This area is one of the recommended areas by Malaysia – West Germany Team in some years ago as to be surveyed in detail. Two geochemical anomalous zones of Cu, Pb and Zn were detected in the stream sediments.

For clarifying the sources of these anomalies, the geological survey and geochemical surveys for stream sediment and soil, were carried out over an area of 4 km².

The geological survey clarified that the type of mineralization is of arsenopyrite vein and pyrite-pyrrhotite dissemination bearing chalcopyrite.

It was clarified by the geochemical survey that a small anomalous zone of Cu, Pb and Zn is located in the central area and the rest areas show low values of Au, Cu, Pb, Zn and Mo in both stream sediment and soil.

PART I INTRODUCTION

CHAPTER 1 OUTLINE OF SURVEY

1-1 Background and Purpose of Survey

The area contains the Mamut mine, a well known operating mine, and various kind of surveys were made in the Area. Regarding geology and ore deposit, the detailed surveys have been carried out, however they are local, naturally centering on the Mamut mine.

The past survey would have to be localized because the main target was the ore deposit, and at the same time, those surveys have not always fully illuminated the relationship between the mineralization, geological structure and igneous activity hindered by a steep topography of Mt. Kinabalu, the highest peak in the Southeastern Asia, and the Pinosk Gravels, the Quaternary glacier mud flow sediment which covers the surrounding part of Mt. Kinabalu.

The purpose of this survey, therefore, is to evaluate the potential for ore deposit by elucidating the geological structure of more high accuracy and grasping the geological environment connecting to the occurrence of ore deposit through various investigations including basic survey for the area selected as the area of ore showings based on the existing data.

1-2 Contents of Survey

1-2-1 Survey Area

The survey area, agreed and signed on June 15, 1985 between the Economic Planning Unit in Prime Minister's Office of Malaysia and the Japanese mission including the preliminary survey team and the agreement and negotiation team, has E-W length of about 52 kilometers and N-S width of about 40 kilometers occupied by Mt. Kinabalu (4,101 m above sea level) in the north-western part (Fig. 1).

This year, the first year of the project, the area selected for survey was divided into subareas such as reconnaissance survey area, semidetailed survey area and detailed survey area according to the method of survey, because there are wide range of potentials for occurrence of ore deposit by area as known clearly from the result of past surveys conducted in connection with the development of the Mamut mine included in the area, and the surveys were to be performed in different accuracy for each kind of area.

The project areas are, as shown in Fig. 2, Located to the north of Ranau, 70 Kilometers east of Kota Kinabalu, the capital city of Saba State.

The following surveys illustrated in Table 1 were carried out in the areas.

1-2-2 Method of Survey

The content of field survey for each area is as follows.

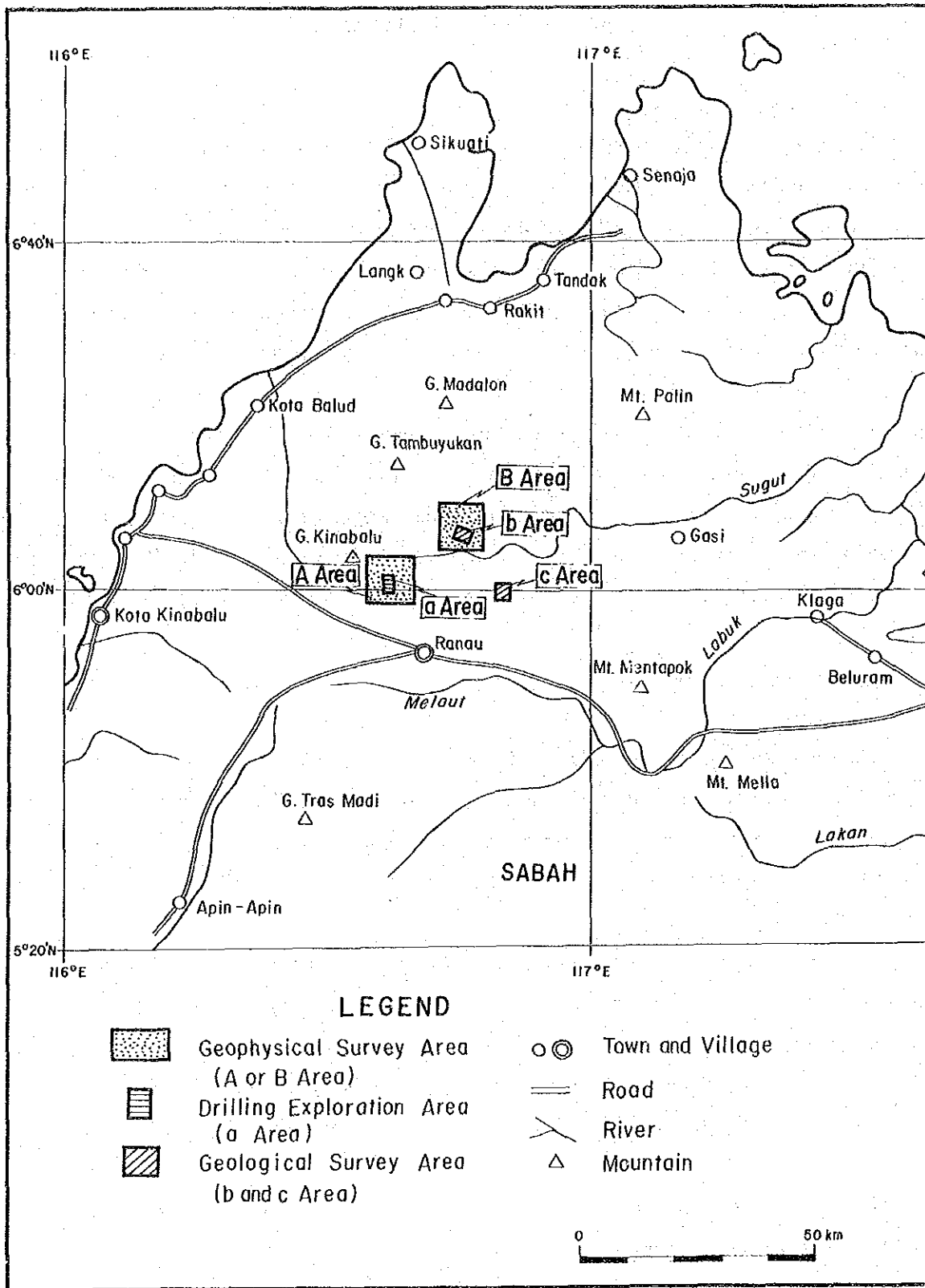


Fig. 2 Location Map of Phase I Area

Geological mapping and geochemical survey

Reconnaissance survey was carried out on a scale of 1 : 2,500 by hand measurement referring to 1 : 50,000 scale topographical map and produced route maps.

Geochemical survey is performed in parallel with geological mapping. In the areas b and c, soil samples were collected in a method of grid sampling for each 50 m x 50 m, and stream sediment samples in the area "c" at an interval of 50 meters.

Geophysical survey (CSAMT method)

The interval between the stations is about 400 meters. In the area A, the stations were filled in for selection of the drill site to be performed in future. The surveys of the area A was made with first priority as compared with other areas.

Measurement was done in grid using the survey lines of geological mapping and geochemical survey.

The stations in the reconnaissance survey area were selected mainly along the ridge or creek so as not to be partial.

Geophysical survey (IP.SIP method)

In the promising area selected from the Area A by geophysical survey (CSAMT method), geophysical survey (IP.SIP method) was conducted along 8 lines, totalling 10.8 kilometers in length (line interval : 200 m, spacing : 100 m, n-factor : 1 ~ 5).

Drilling

The drilling survey of this year was conducted in the area which is close to the Mamut mine to investigate the possibility of the existing ore showings and the promising anomalies to be detected by geophysical survey.

The drilling was made for one 400-meter hole, seven 350-meter holes and two 300-meter holes, ten holes 3,450 meters in total.

1-3 Organization of Mission

The mission of the project includes the members involved in the planning and negotiation, those in the negotiation and investigation for the survey of the first year, and those participated in the field survey of the first year, as shown in the following.

Planning and negotiation

Japanese Counterparts :

Makoto Ishida

Takeshi Nakayama

Hideyuki Ueda

Kojiro Komura

Metal Mining Agency of Japan (MMAJ)

MMAJ

Japan International Cooperation Agency

Agency of Natural Resources and Energy

Michihisa Shimoda	MMAJ
Atsushi Osame	MMAJ
Yasuo Endo	MMAJ

Malaysian Counterparts :

Yin Ee Heng	Geological Survey of Malaysia
Dato Seri Radin Soenarno Al-Haj	Economic Planning Unit
David Lee Tain Choi	Geological Survey of Malaysia, Sabah

Field Survey

Japanese Team :

Hajime Shimizu (Leader; geology, geochemistry, core inspection, report)	Bishimetal Exploration Co., Ltd. (BEC)
Hiroshi Fuchimoto (Geology, geochemistry)	BEC
Hisao Takeda (Geology, geochemistry)	BEC
Tadashi Yamakawa (Geology, geochemistry)	BEC
Tomio Tanaka (Geophysics)	BEC
Kohei Sugawara (Geophysics)	BEC
Kazuto Matsukubo (Geophysics)	BEC
Tomie Tozawa (Drilling)	BEC
Toshio Murayama (Drilling)	BEC
Mitsuru Ambo (Drilling)	BEC
Koji Kudo (Drilling)	BEC
Mahito Hamazaki (Drilling)	BEC
Isao Matsuoka (Drilling)	BEC
Hiroshi Saito (Drilling)	BEC

Malaysian Team :

Lim Peng Siong (Supervising, report)	Geological Survey of Malaysia, Sabah (GSM)
Tungah B. Surat (Geophysics)	GSM
Mohd Yusof Ramli (Geology, Geochemistry)	GSM
Chan Fook On (Chemical Analysis)	GSM
Technical Assistants –	
Kwan Houng En (Geology, geochemistry)	GSM
Kirman B. Sukard (Drilling)	GSM
Salleh Adanan (Geology, geochemistry, geophysics)	GSM
Roger Jinijo Totu (Geophysics)	GSM
Kamil Kamaruddin (Drilling)	GSM

Table 1 Outline of Field Survey in Phase I

	Duration	Survey Figures		Remarks
		Area	Length	
Preparatory Work	Aug. 8 ~ 16, '85 9 days	-	-	
Geological & Geochemical Survey	Aug. 17 ~ Oct. 24, '85 69 days	b ... 4 Km ² c ... 4 Km ²	85.2Km 117.7Km	Soil Samples b...1681 pcs c...1681 pcs Stream Sediments b... 665 pcs
Geophysical Survey	Sept. 28 ~ Dec. 1, '85 65 days Apr. 3 ~ May 24, '86 52 days	A... 100Km ² B... 100Km ²	204 Stations 5.4Km 5.4Km 203 Stations	CSAMT Method SIP Method IP Method CSAMT Method
Drilling	Sept. 21, '85 ~ Aug. 7, '86 321 days	MJM-1 -2 -3 -4 -5 -6* -7 -8 -9* -10	305.30 m 351.00 m 300.50 m 351.00 m 350.60 m 302.60 m 350.20 m 351.00 m 401.10 m 351.90 m 3,460.20 m	Inclination * -90° Others -50°

CHAPTER 2 GEOGRAPHY OF SURVEY AREA

2-1 Location and Accessibility

The survey area is situated in Sabah State among the two states of East Malaysia.

Sabah State is opposite on the north to Parawan Island of the Philippines with Balabac Strait between. The state is connected by land on the south with Kalimantan of Indonesia, Brunei, a newly emerging nation, and Sarawak State of the Federation. Sabah State is situated on the northwestern most end of Borneo Island, the third large island in the world, and has an area of about 76,000 square kilometers, nearly equal to that of Hokkaido of Japan.

The survey area is centered on the town of Ranau (with population of about 2,000), having an extent of 52 km in E-W by 40 km in N-S (Fig. 1).

Mt. Kinabalu (4,101 meters above sea level), the highest mountain in the southeastern Asia, is situated in a little northwestern part of the survey area.

Kota Kinabalu is at 116° East Longitude and 6° North Latitude.

The area surveyed in the first year is on the north of the downtown of Ranau (see 1-2-1 Survey Area).

It takes two hours by car to reach Ranau from Kota Kinabalu by the sealed road. Beyond there to the survey area, however, the roads are unsealed and rough. In addition, absence of bridge over the rivers and creeks often causes to cut off all the communication by flood of streams when heavy rainfalls, leading to difficulties of maneuvering.

In usual case, it takes within an hour by four wheel-drive car to reach the entrance of the survey area from Ranau (the air flight service between Kota Kinabalu and Ranau has been suspended, and the air strip at Ranau has not been used at all, and remains untouched without any maintenance.)

The access by car is partly possible in the survey areas, however most of the surveys in the first year was done on foot.

2-2 Topography

The Crocker Range runs northeasterly along the coast facing the South China Sea on the west, which strongly control the topography of Sabah State, in which the highest peak of Kinabalu shows an altitude of 4,101 meters. But the mountains are mostly 900 to 1,500 meters in height.

At the foot of the western slope of the range, an alluvial plain about 10 kilometers wide forms the coastal zone, which sometimes continues to the low coastal mangrove swamp.

An extensive highland, 200 to 1,000 meters high above sea level, is distributed on the eastern side of the Crocker Range, through which large rivers in Sabah State running toward the east form lowlands, flowing into the Celebes Sea through the low mangrove swamp at the mouth of the rivers.

The area "A" is situated on the southeastern slope of Mt. Kinabalu where an adamellite intrusive mass forms a peak at the center of the area, forming a steep slope from an altitude of about 3,600 meters toward the south.

A conspicuous fault scarp runs with the trend of E-W showing a difference of altitude between the upper edge of 2,000 meters and the bottom of 1,300 meters. The south is a hilly terrain of relatively gentle slope distributed by the Tertiary sediments, which shows an extensive distribution further on the east reaching up to Ranau at the bottom of slope, forming a plateau covered by the thick beds of the Pinosuk Gravels consisting of glacier sediments and mud flow sediments.

Rapid streams rising from the Kinabalu mountain mass flows engraving the plateau toward the east or south, selecting the soft sediments, and forms deep valleys with steep cliffs on both sides.

The area "a" which is selected for drilling and semidetached geophysical survey, occupies an area of valley along the Bambang creek, one of the rapid stream.

The area "B" is in the central highland on the eastern side of the Kinabalu mountain mass, apart from the range. Although a height of 1,300 meters is shown at its western periphery, the elevation is lowered toward the east where the rapid streams engraving the Kinabalu mountain mass slow down the speed of current coming into the plateau, forming locally the dissected plateau, being lowered to about 250 meters above sea level in the vicinity of Paranchangan village in the northeastern part of the Area. While the area "b" is relatively low in elevation (550 to 300 meters above sea level), the northeastern half of the area shows a steep landform with basalt and the basic rocks distributed on the west. Further on the west, bordered by the River Sansogon, a tributary of the Mankadau River flowing southeastward along the fault and in its extension, the sedimentary rock is distributed forming a flat landform.

The area c is the detailed survey area for geological mapping and geochemical survey. Though small in area, two peaks of the dioritic intrusive rock are protruded, showing a very steep landform in the surrounding area (often steeper than 50 degrees in inclination of the slope), having led to the difficulty of survey.

The sedimentary rocks on both sides are dissected in many parts to form V-shaped valley by rapid stream rising from the intrusive peaks. The steep slopes in the sedimentary rocks become

gentle toward the southern margin of the area, where a soft landform is shown.

2-3 Climate and Vegetation

Climate in Sabah State is tropical and oceanic, and also the area belongs to the monsoon district. However, the variation in precipitation by season is small except for a part of the coastal zone. From October to March, the monsoon blows from the northeast, and from May to August from the southeast. Therefore, it rains relatively heavily in the coastal zones in the seasons, in which the wind is against.

The annual precipitation in the mountainous area of inland is 1,500 to 2,000 millimeters, and it is more than 3,000 millimeters in many areas of coastal zone and in the mountain. The annual precipitation at the Manut mine is shown to be 2,100 to 4,000 millimeters (Table 2).

No seasonal variation of temperature is clearly observed, and it is shown to be 24° to 30°C with the maximum of 34°C in the coastal area, and 12° to 22°C in the mountainous area, showing a notable daily variation in the latter.

The vegetation on the hill and in the mountain is so-called the jungle type, and the coastal area is generally represented by the swampy zone where mangrove grows thick. All the survey areas are the zone of jungle in which tall and dwarf trees, herbaceous plants and ferns grow very thick because of much moisture, leading to take time for clearing the route for the survey.

Table 2 Records of Monthly Rainfall

Year 1975 - 1985

Ranau Agricultural Station
549 Metres AMSL 5° 58'N 116° 42'E

YEAR	JAN.	FEB.	MAR.	APR.	MAY	JUN.	JUL.	AUG.	SEP.	OCT.	NOV.	DEC.	TOTAL	WET DAYS
1975	374.3 17 Days	158.7 7	170.9 10 10	80.3 7	296.1 17	189.5 13	257.0 18	324.3 15	208.8 19	226.5 9	203.4 19	195.8 17	2685.6	168
1976	279.4 18 Days	72.1 8	121.2 9	117.2 8	57.9 5	97.3 8	84.3 7	195.9 10	55.5 5	252.0 17	213.6 18	160.3 9	1706.7	122
1977	236.6 12 Days	615.1 18	71.3 9	126.9 10	199.8 13	289.9 17	101.3 12	264.3 11	70.1 5	253.7 13	213.0 11	126.8 16	2568.8	147
1978	185.4 11 Days	122.4 7	82.8 4	227.0 10	184.7 10	288.2 17	140.0 13	72.4 4	169.7 7	170.4 15	96.0 12	268.6 20	2007.6	130
1979	101.4 16 Days	88.5 9	170.0 13	88.7 6	195.5 13	177.1 16	192.1 12	44.0 7	181.2 12	221.0 13	265.2 19	81.0 8	1805.7	144
1980	237.8 18 Days	229.6 11	214.0 11	122.0 11	139.3 9	133.7 14	225.3 11	166.3 15	107.7 6	140.7 13	105.1 12	362.9 21	2184.4	152
1981	556.4 22 Days	148.2 10	86.1 6	84.8 7	-	73.8 7	131.5 13	113.8 6	164.3 14	168.8 9	148.4 11	129.1 11	1805.2	-
1982	253.2 12 Days	124.6 13	79.8 4	138.4 11	278.0 16	193.4 10	124.5 10	112.4 15	220.7 10	122.6 12	136.1 13	100.6 10	1884.3	136
1983	102.3 8 Days	61.4 6	0.0 0	1.3 1	160.3 6	266.6 16	172.2 12	391.5 22	205.8 19	119.7 14	190.4 14	301.0 24	1972.5	142
1984	256.7 24 Days	368.0 26	138.5 15	245.5 19	362.6 23	197.0 14	430.8 17	26.4 5	221.9 18	79.1 10	147.2 16	284.1 23	2757.8	210
1985	152.5 6 Days	301.7 17	48.6 7	140.9 11	175.8 11	109.0 8	175.4 11	192.6 11	212.8 17	155.4 12	178.7 18	92.0 11	1935.4	140

Remarks: -, not available

CHAPTER 3 GENERAL GEOLOGY AND PREVIOUS SURVEY

3-1 Geology of Sabah Region

Geographically, Sabah State is situated in the northern part of the Borneo Island, and the area selected for the collaborative survey is located in the western part of the state.

From regional view point of geology of the area, a geosynclinal and orogenic zone including the late-Cretaceous to the whole Tertiary formations more than 800 kilometers long and 300 kilometers wide are distributed trending northeasterly in the northwestern part of the Borneo Island extending from the western half of Sabah State through Brunei on the southwestern side to Sarawak State. This zone is called the "Northwest Borneo Geosyncline (Haile, 1969)" (Fig. 3).

It is said in recent years (after 1970's) that a "large concentration of copper" (porphyry copper type) would have taken place in zones confined to the convergent part of the plate based on the theory of plate tectonics which can be related to the formation of porphyry copper deposit.

The history of orogenic movement of the region has not been explained plainly due to the complicated geological structure and the bending structure in a form of letter Z, because the northeastern side of Sabah State provided the field of island arc collision by the stress from the Sulu Sea.

The intrusion of the batholithic rocks which formed the Kinabalu mountain located in the center of the survey area is also the product of the complicated orogenic movement, making the elucidation of mineralization of the area more difficult.

The northwest Borneo geosyncline is conspicuous with the distribution of spilite extrusives in late Cretaceous, the sedimentary rocks and the Rajang Group composed of flysh-type sediments (Eocene to Early Miocene), the product of the geosyncline.

The igneous activity includes intrusion of ultrabasic rocks belonging to Cretaceous and intrusion of plutonic rocks during and after the orogenic stage (middle Miocene to Pliocene) followed by the extrusion of andesite and basalt. That is, the geology of a series of typical geosynclinal orogenic movement and the structure are shown.

There is an extensive zone of tectonic lines of a NW-SE system (a group of faults of middle to small scale more than 100 kilometers wide) which includes the Kinabalu mountain mass, and it is called the "Kinabalu faults" (Tokuyama and Yoshida, 1974). The Rajang Group is displaced greatly by this zone, and numerous acidic and ultrabasic intrusives and extrusives are found in

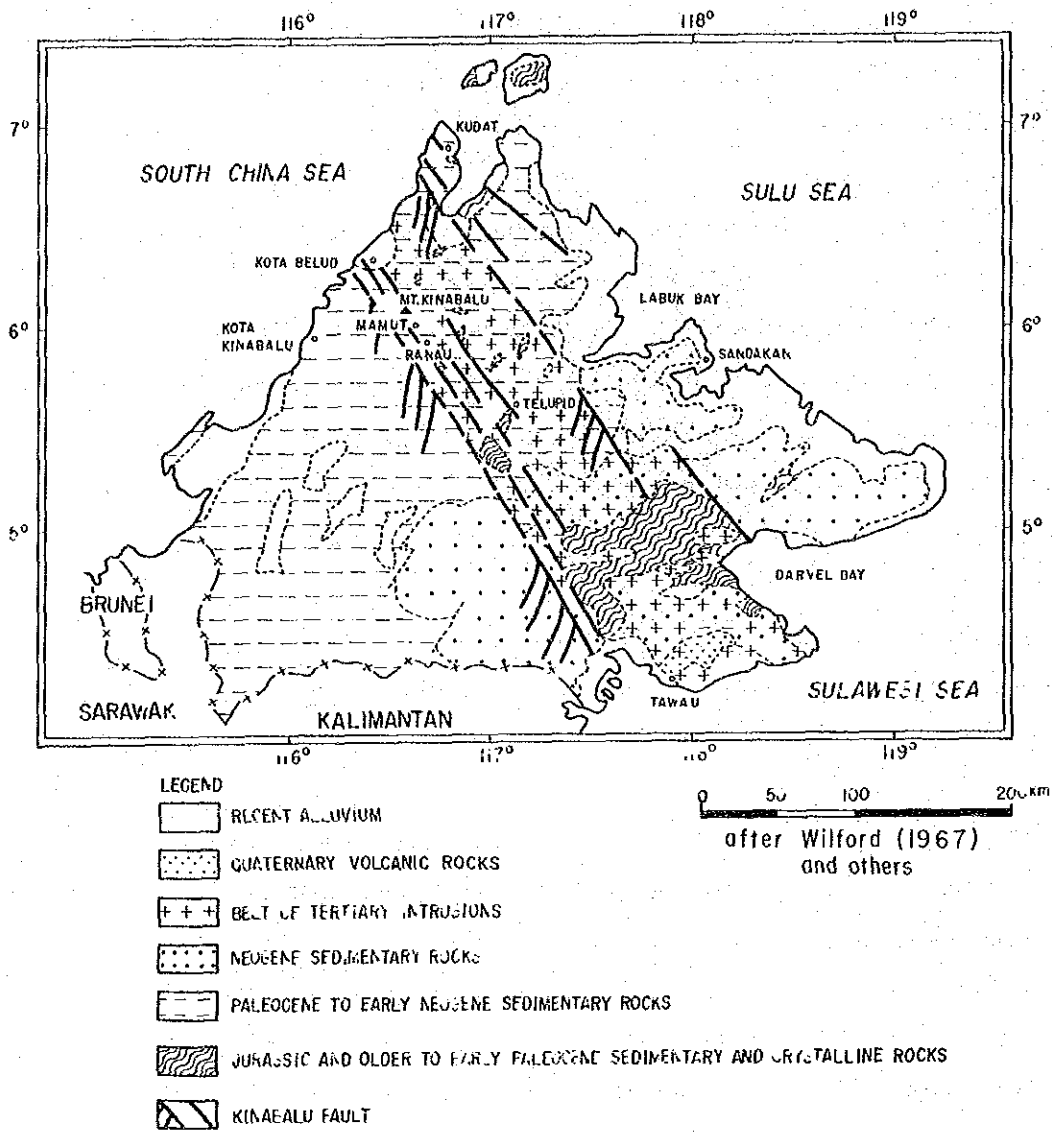


Fig. 3 Generalized Geological Map of SABAH

the zone.

The rocks thought to form the basement are schists and gneisses called the "Crystalline Basement" belonging to Jurassic or the time earlier than that, which are known to be distributed locally in the survey area.

The igneous activity after the basement is compiled by Kirk as follows.

Igneous activity of the first stage :

This is the submarine basic igneous activity rich in sodium, including spilite and keratophyre in the early stage of geosyncline. The main rocks include the basic igneous rocks in the chert-spilite formation distributed in the eastern and northern parts of Sabah State and spilite pillow lava in the central part. The former is the result of activity of Cretaceous to Eocene and the latter that of early Miocene. The spilite group and the ultrabasic rocks are distributed almost in the same area showing the trend of northwest to southeast in Sabah State.

Igneous activity of the second stage :

This activity includes those of acidic to intermediate, such as the Kinabalu mountain plutonic mass and the intermediate intrusive rocks of small scale surrounding the mass, which intruded in late Miocene to early Pliocene (immediately after the orogenic stage). The volcanic activity mainly of andesite and dacite, which are almost contemporaneous to the above, took place in the area on the eastern side.

The latest volcanic activity of the North Borneo geosynclinal stage was shown in extrusion of the Pleistocene basalt lava. (Fig. 4).

3-2 Geological Setting of Project Area

The intrusive batholith of adamellite is distributed protruding in the surface slightly extending northeasterly, with an area of 155 square kilometers (60 square miles), showing a peculiar landform with an altitude of 4,101 meters above sea level, which is said to be spread over 1,300 square kilometers (500 square miles) in subsurface (Jacobson 1970). Therefore, it would be distributed both on the surface and underneath of the whole extent of the survey area as batholith. The peripheral part of the rock becomes porphyritic, and it is distributed surrounding the Kinabalu mountain mass as adamellite porphyry, especially dominantly on the southern and western sides of the mountain in a zonal form. It is also exposed on the northern side of the Poring settlement to the east of the mountain mass forming a low mountain mass (about 750 meters in altitude) slightly extending northeasterly (Fig. 5, Fig. 6).

Because the whole area of Mamut ore deposit which is adjacent to the Kinabalu mountain mass on the southern side is considered to lie over the batholith in subsurface, the stocks

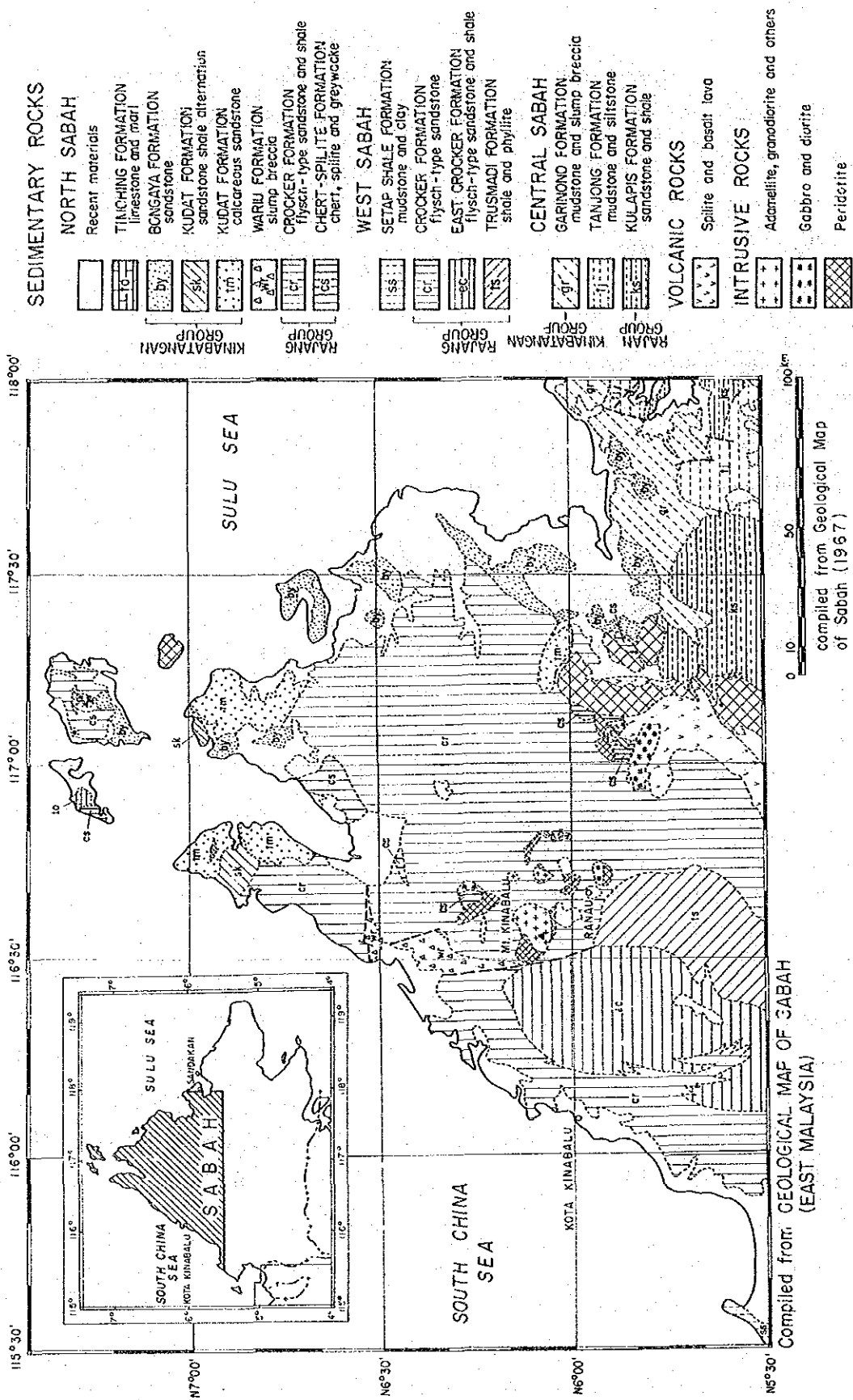
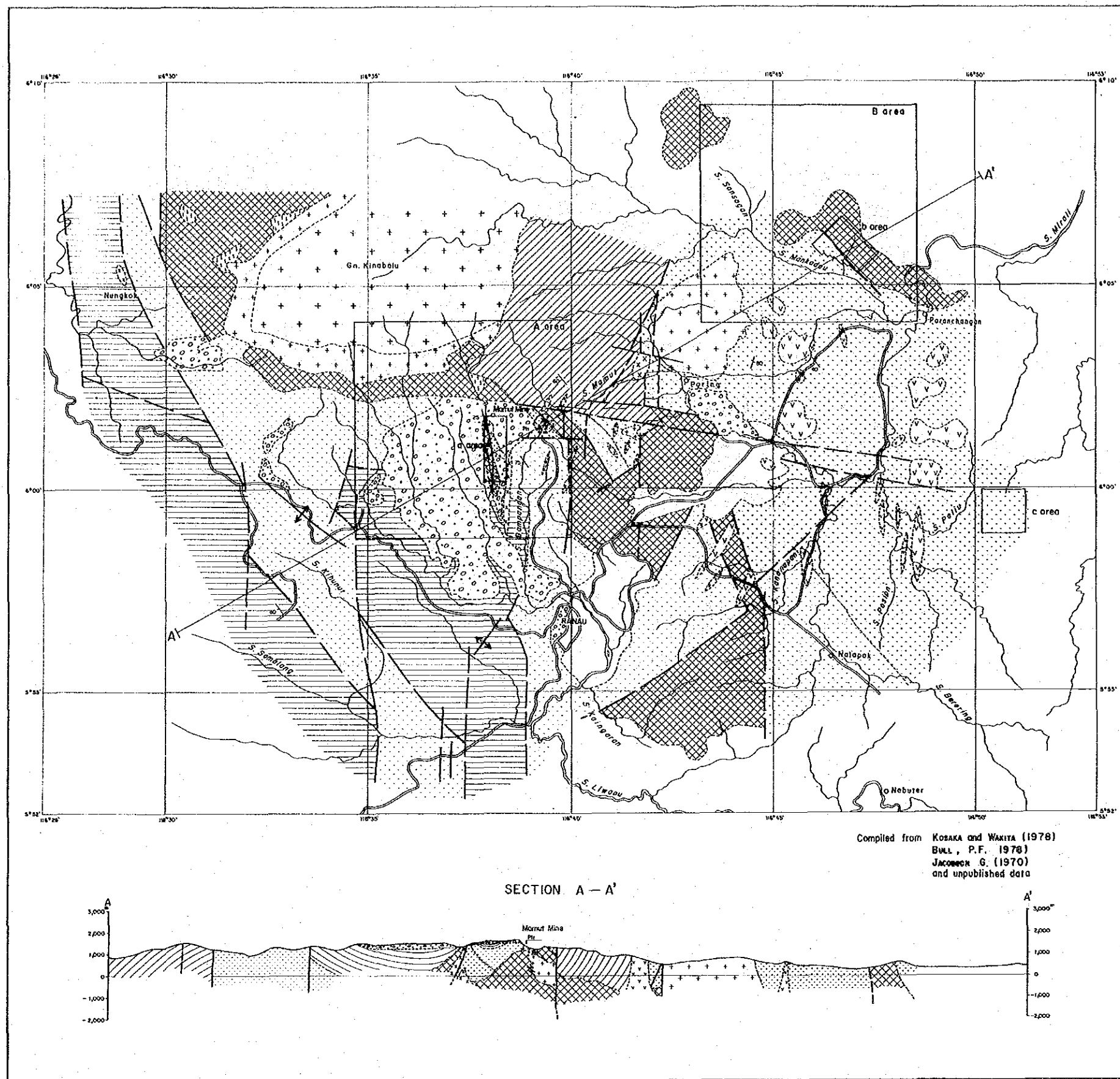
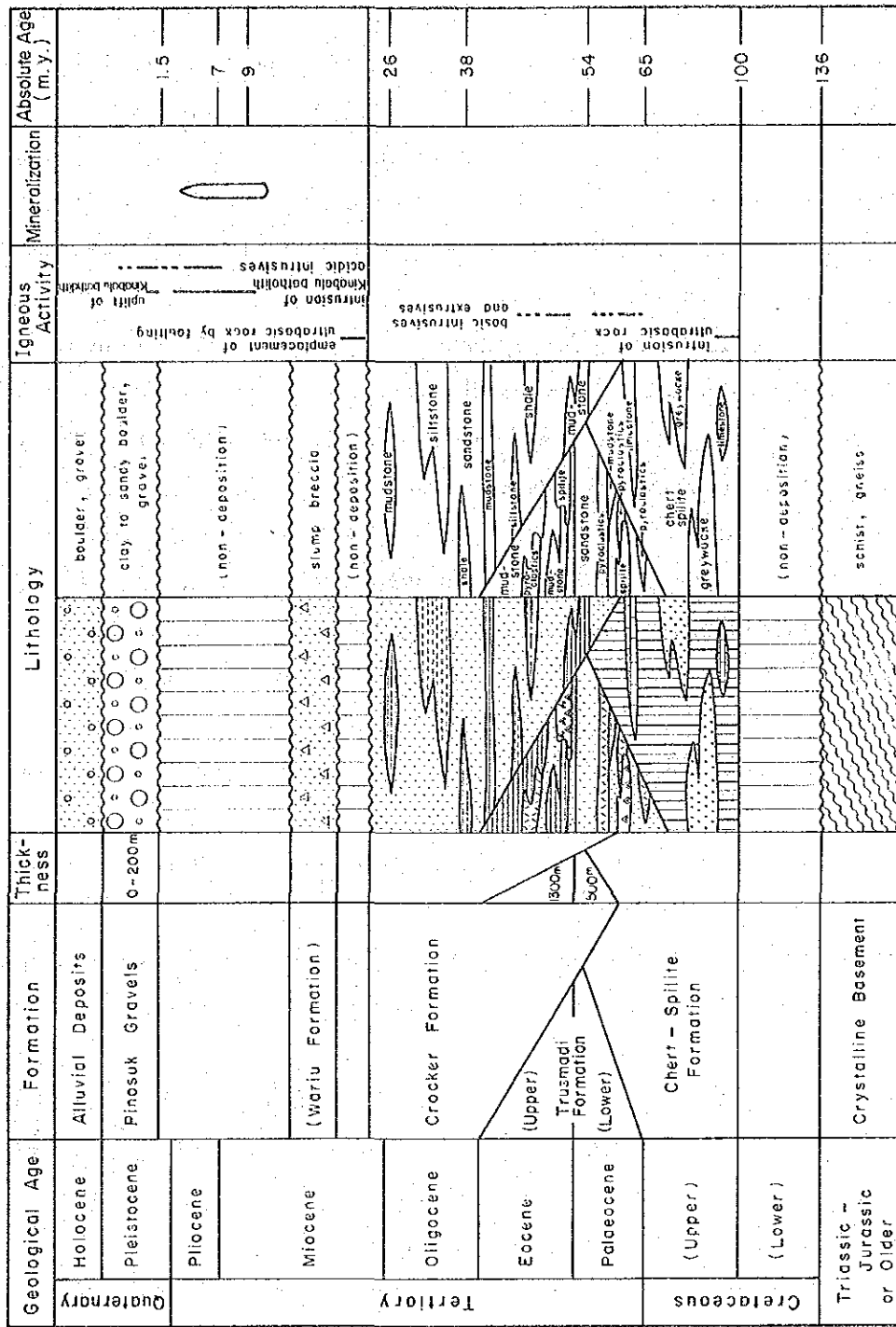


Fig. 4 Geological Map of West SABAH



- LEGEND**
- Alluvial deposits
 - Pinok Gravels
 - Boulders and gravels
 - Crocker Formation
 - Sandstone, siltstone and mudstone
 - Trusmi Formation
 - Sandstone, mudstone and spilite and its pyroclastics
 - Sandstone, mudstone and spilite and its pyroclastics
 - (unknown) Undifferentiated sedimentary and metamorphic rocks
 - Crystalline Basement
 - Schist and gneiss
- Igneous Rock**
- Andesite and dacite
 - Microdiorite and Micro quartz diorite
 - Adamellite porphyry
 - Adamellite
 - Serpentinized peridotite
- Fault (certain) Fault (inferred)
- Strike and dip Anticline
- Geological profile line
- Survey area

Fig. 5 Geological Map of KINABALU Area



(Compiled mainly from Kosaka and Wakita, 1975)

Fig. 6 Generalized Stratigraphic Section of Survey Area

of adamellite porphyry (about 800 meters in N-S and 300 meters in E-W, dipping 40° eastward in general; Kosaka and Wakita, 1975) which is widely distributed within and in the vicinity of the ore deposit, forming the main host rock of the deposit and having been directly involved in the mineralization, and the dykes observed in abundance on the top and in the peripheral part of the stock, are all the cupolas or apophyse branched off from the Kinabalu adamellite batholith.

The rocks which form the basement of the Tertiary sedimentary rocks is the "Crystalline Basement" consisting of schists and gneisses as mentioned previously, and their ages are classified as Jurassic and Triassic, or earlier than Jurassic.

The sediments deposited overlying the Crystalline Basement are represented by the Chert-Spilite Formation composed of chert, spilite and the sedimentary rocks, and the Rajang Group composed of flysh-type sediments. The former belongs to the late Cretaceous to Palaeocene sediments and the latter to the Palaeocene to early Miocene.

The Rajang group is divided into the two formations such as Trusmadi and Crocker. In connection with their age, although the Trusmadi Formation has been classified as Palaeocene to Eocene, and the Crocker Formation as the later (Oligocene to early Miocene) for the time being, the stratigraphy of the two formations has not yet been established because of complexity of geologic structure of the area.

Lithologically, the Trusmadi Formation consists of grey to dark grey argillite and slate, and partly siltstone with rare occurrence of pyroclastics.

The Crocker Formation is rather arenaceous as compared with the Trusmadi Formation, being composed of sandstone, siltstone and gray or red shale.

It is said that there are some areas in which the Chert-Spilite Formation shows the lateral gradation with the upper Trusmadi Formation as contemporaneous heterotopic facies, and it can be said that the stratigraphy of the area has not yet been established.

The sedimentary rocks distributed in the lowland on the southern side of the ultrabasic rocks in the area "b", selected for the survey of the first year, has been classified as the Trusmadi Formation. It seems, however, that those sedimentary rocks rather belong to the Chert-Spilite group from the relationship with the upper spilite basalt lava.

As to distribution of the Rajang Group, the area on the eastern side of the N-S line connecting the Mamut deposit and Ranau is almost occupied by the Trusmadi Formation, and the sedimentary rocks including those of the lower part of the Pinosk Gravels widely distributed from the N-S line to Kundasang on the west which will be mentioned later, and those extensively distributed around Mt. Nungkok which forms a small mountain mass of adamellite to the west of

the Kinabalu mountain mass, are classified as the Crocker Formation.

It is evident from the observation of complicated distribution of the Crocker Formation between Ranau and Kundasang along the many cuttings of the main road leading to Kota Kinabalu that the two formations have a complicated geological structure by repetition of folding and faulting. The sedimentary rocks which form a part of the wall rocks of the Mamut ore deposit are classified as the Trusmadi Formation.

The sedimentary rocks (partly include metamorphic rocks) widely distributed on the northern side of the easterly trending fault in the M-1 area forming the northern border of the Mamut ore deposit was once classified as the Trusmadi Formation (before 1970), but it is classified as undifferentiated sedimentary and metamorphic rocks at present, without establishment of clear stratigraphical classification.

These formations are metamorphosed by intrusion of the Kinabalu batholith, especially the Trusmadi Formation is subjected to contact metamorphism at the contact on the eastern and southern sides of the mountain mass, and the peripheral zone of the formation reaching up to 1,500 meters from the contact has been altered to hornfels, schist or quartzite. This phenomenon can be observed along the Bambang creek in the sedimentary rocks in the area of drill survey.

From the view of standpoint of geological history, the ultrabasic rocks are the first of the intrusive igneous rocks of the area, and the Kinabalu plutonic rocks intruded in the later stage.

The ultrabasic rocks in the survey area are distributed on the southern side and the western side of the adamellites of the Kinabalu mountain mass, in the area "B", in the southeastern part of Mamut and on the southwest of Ranau. The rock consists mainly of peridotite, and dunite is observed locally. These rocks have been sheared and fractured to produce breccia in many cases. Serpentinization is generally observed.

In Sabah State, the ultrabasic rocks are often distributed in contact with spilite lava, and they show a wide distribution being in contact with the spilite basalt lava on the southern side of the fault laid between them. Adamellites constituting the Kinabalu mountain mass have been dated to be 9 m.y. of absolute age, corresponding to the later stage of the orogenic movement which took place from late Miocene to Early Pliocene, or immediately after that age. According to Jacobson (1970), adamellite intruded into the ultrabasic rocks showing a vertical contact (western bank of the Bambang creek).

The Kinabalu mass itself is composed of adamellite, and porphyritic adamellite and adamellite porphyry in the marginal part. It is the same in the cupolas in the surrounding area of the mass. In the Mamut area, intrusion of these cupolas resulted in forming a dome structure both in

the ultrabasic rocks immediately above the cupola and the sedimentary rocks overlying them.

In the Mamut mineralized zone, the presence of granodiorite porphyry dyke is known to form a very small part of the ore deposit, clearly cutting adamellite porphyry. Therefore, it is later than adamellite porphyry which is closely associated with the Mamut mineralization, but it has been subjected to mineralization (although copper grade is about one-third that of those host rocks such as adamellite, ultrabasic rocks and sedimentary rocks), and seems to be the intrusive rock in the later stage of a series of plutonic activity of the Kinabalu adamellite intrusive mass.

Beside these, microdiorite is found mainly as N-S trending dykes around the Mamut ore deposit area, which has not been found on the surface of the deposit. This rock corresponds to Por-2 among those described as the porphyritic rocks (hypabyssal porphyritic rock) (OMRD's report on investigation of the Mamut ore deposit, January 1971) (Por-1 corresponds to adamellite porphyry which is the main host rock of the mamut ore deposit. Por-2 was encountered in the drill hole MJM-1 and MJM-3 in the survey of this project, having continued for about 220 meters), and shows porphyritic texture with distinct phenocryst of garnet (the hole MJM-1 and MJM-3 was drilled in close proximity of the hole BA-1 of OMRD's survey project in 1971). Although the time of intrusion of the rock has not been made clear, it might be considered to be in the later stage of activity of the Kinabalu plutonic intrusion and also in the later stage or final stage of the mineralization associated with it.

On the eastern side of the survey area, dacite and andesite are distributed in the Trusmadi sedimentary rocks which shows a wide distribution, having intruded and extruded as stocks and dykes, or partly as lava. These are thought to represent the later stage of the Neogene Tertiary igneous activity.

The one of unexpected obstacles for the survey activity in the area was the Pinosuk Gravels, the Quaternary sediment, although it is not related to the Tertiary orogenic movement, igneous activity or mineralization.

This bed is distributed for an extent of about 50 square kilometers at an altitude between 1,500 and 1,200 meters on the southern side of the Kinabalu mountain from the upper flank of the relatively gentle slope, where a steep landform of the intrusive mass comes to an end, toward the south through the Pinosuk settlement, which gave the name of the bed as type locality. The lower end of it collapsed and flowed out as mud flow to reach the Ranau floodplain on the southeast, and the great boulders have remained in the riverbed of the large and small rivers flowing at the periphery and in the alluvial floodplain of the Ranau basin.

The kinds of pebbles and boulders include all the rock kinds constituting the geology of the

area such as adamellite, adamellite porphyry, ultrabasic rocks and the Tertiary sedimentary rocks, and naturally, sometimes the pebbles of mineralized rock are contained.

The size of the pebbles varies widely from 1 to 50 centimeters to 1 to 5 meters, rarely reaching up to 10 to 20 meters. They are generally subangular and sometimes breccias and rarely round pebbles are found.

The groundmass mainly consists of coarse-grained sand of adamellitic origin, and the grade of consolidation is varied.

The radiometric carbon age on buried wood has provided $7,980 \pm 100$ years for the uppermost part, and 34,000 (+2,000 ~ 1,800) years and 39,900 + years for other parts, leading to the assumption of the age of the later Quaternary.

Jacobson (1970) divided the bed into two sections by the unconformity plane based on the genesis, and defined the lower section to be the conglomerate formed by periglacial phenomena at the time of ice age of the Kinabalu mountain, and the upper section the sediments of mudflow from high mountain, partly containing reworked moraine of glacier.

Faults of a N-S system in the area are dominant, which are divided into sections by the faults of NW-SW system to form blocks. And the block movements were repeated, in which the outside (southern side and eastern side) blocks slipped down on the eastern and the southern sides of the Kinabalu mountain mass.

Faults of a E-W system and a NE-SW system are also present, and they control the local structure, though small in scale as compared with those in the above. For example, weak fracture zones of a NE-SW system are developed in a form of echelon, and the overall ore zones take a northerly extending form. The fault bordering the northern limit of the deposit is notable among E-W system faults, cutting adamellite porphyry, and the southern block slipped down against the northern block. These faults are considered to be related to the uplifting of the Kinabalu Mountain and the movement would have continued from the initiation to the final stage of the mineralization.

3-3 Previous Surveys

1882 : F. Hutton made a reconnaissance survey over the Tambuyukon mountain area, and confirmed the distribution of pyrite.

(Hutton F., North Borneo exploration and adventure on the equator, London 1885)

1908-1912 : British Borneo Exploration Company conducted a systematic investigation on mineral resources of North Borneo.

(R.R. Pily, Geologische Studium im Britische Nord Borneo, Jahresher Freiberge Geol. Ges. VI 1913)

1949 : In the wake of establishment of North Borneo Geological Survey, the basic and general investigation on geology and ore deposit was started.

1955–1956 : The Sabah Geological Survey performed geochemical survey in the Karang area of Telupid with cooperation from Royal School of Mines (London), and it was recognized that geochemical survey had been effective in jungle. (Mémair 9).

1958 : F.H. Fitch completed the geological map of Sandakan-Labuk Quadrangle (Memoir 9), and emphasized the need of geochemical survey in the Labuk area.

P. Collenette completed the investigation on general distribution of geology and mineral resources in the Jesselton (Kota Kinabalu at present) – Kinabalu area.

(Collenette P., The Geology and Mineral Resources of Jesselton-Kinabalu Area 1958)

1959 : Soriano Y. Cia obtained the prospecting right on Au, Cu, Pb, Zn and Ni (1,118 mile²) in the areas such as Tambuyukon, Karamuak and Darvel Bay.

1960 : Soriano Y, Cia obtained the prospecting right in the Karang area (1,000 mile²).

1962 : Sabah Geological Survey recognized the occurrence of cinnabar by panning on the downstream of a stibnite outcrop at Randagong (southwest of Ranau).

Malayan Mines Ltd., obtained the mining right of 29 mile² at Bidu-Bidu Hill.

Borneo Mining Ltd., conducted drilling at Bidu-Bidu in the Labuk area for exploration of chromium. The drilling was also made on the iron ore deposit discovered by the quadrangle geological mapping of the Geological Survey at the Tavaj mountain in the Labuk area, and a considerable amount of ore reserve was confirmed.

Soriano Y. Cia started exploration of copper deposit of various areas in Saba State. Geochemical Survey was carried out in the Karang-Karamuak area, resulting in detection of copper anomalies in the northern part of the Mankadau area in the Tabuyukon area, and boulder of copper ore was discovered in the rivers such as Sansogon and Lingangaa, then the mineral lease was established in the area.

1963 : The Labuk Valley Project was conducted. At first, reconnaissance geochemical survey was started in the Labuk-Karamuak area by the special fund of the United Nation.

Soriano Y. Cia continued geochemical survey by stream sediment of regional scale, and in addition, carried out geoelectrical survey and pitting in the Mankadau area. However, the prospecting was suspended by the failure to find out massive copper deposit as seen on the outcrop.

(September 16, 1963, the Federation of Malaysia became independent)

1964 : Soliano Investment Co., (successor to Soriano Y. Cia) detected the anomalies of geochemical and electrical surveys at the prospect of Karang in the Karamuak area. Further, floats of boulder of copper ore were discovered at Nungkok by reconnaissance geological survey in the Kinabalu mountainous area. Reconnaissance geochemical survey (640 mile²) was conducted in the Karamuak area, following the survey of the previous year. The follow up survey was started on the copper anomaly in the Sualog and Bangau areas on the Bidu-Bidu Hill (Annual Report 64).

The Sabah Geological Survey indicated the possibility of occurrence of ore deposit in the Kinabalu area at the time of geological mapping for the quadrangle geological survey by finding out quartz boulders containing chalcopyrite.

1965 : Soriamont Investment Company newly obtained the prospecting right (60 mile²) in the Nungkok area and conducted geological mapping and geochemical survey, having resulted in to discover the copper mineralized zone (in silicified mudstone intruded by quartz diorite) on the western slope of Mt. Nungkok.

Labuk Valley Project (United Nation) :

Reconnaissance geochemical survey was conducted, having detected eight copper anomalous areas including M-1 and M-2. Among these, M-1, M-2 and Bambang areas were investigated for follow-up survey (Annual Report 65).

The Sabah Geological Survey conducted geological mapping of the Mamut (M-1 and M-2) and Bambang areas which had been investigated by the United Nation for the follow-up survey among the geochemically anomalous zones detected by the Labuk Valley project, and recognized the occurrence of porphyry copper in the upper reaches of M-2.

1966 : Soriamont Investment Company continued the exploration in the Nungkok area and performed the electric survey and drilling of five holes in the extent of 1,000 m x 400 m. The Sabah Geological Survey conducted drilling of 30 shallow holes and excavation of more than 200 pits centering on the M-2 area, having confirmed the copper mineralized zone of 0.7 per cent in grade over an extent of 150,000 square meters. The exploration by pitting and auger drilling in the Bambang area resulted in not to warrant economical development of the deposit.

Meanwhile, the Sabah State Government decided to invite international tenders for the mining right of the Mamut and Bambang areas (Annual Report 66).

1967 : Soriamont Investment Company continued the exploration of the Nungkok area (two drill rigs), which was suspended without confirmation of the ore reserve to warrant econom-

ical development.

The OMRD (Overseas Mineral Resources Development) Company made a successful bid for the mining right of the Mamut and Bambang areas of 50 square miles in December after severe competition with the major mining companies of the world.

1968 : The OMRD Co. conducted the exploration of the first phase (land survey, geological mapping, electrical survey and drilling) from April to November.

The exploration of the second phase (drilling and tunneling) was started in December.

1969 : The exploration of the second phase was completed in November.

At the same period, OMRD established the OMRD-Sabah Company in May. The Mamut Mine Development Co., Ltd. was established in December in Japan, which was to be in charge of the feasibility study of the development plan of the mine.

1973 : The mining right was authorized to OMRD-sabah. The development works were commenced.

1975 : In May, the operation of the Mamut mine was started.

1968-69 : Jacobson, C. carried out detailed geological mapping of the Kinabalu area on a scale of 1:50,000 from 1968-1969. His work was published as Report 8 which gives an account of the geology, structure, geological evolution of Mount Kinabalu and mineralization of the area.

1971 : Tokuyama, A. and Yoshida, S. studied the structures of the Crocker Formation in the Ranau-Kinabalu area in 1971. They postulated the existence of the strike-slip Kinabalu Fault.

1978 : Leong, K.M. studied the occurrences of metamorphic rocks (garnet amphibolite, garnet corundum amphibolite, glaucophane-talc schist) of Sabah, including those in the Ranau area in 1978. He postulated the Blueschist belt of Sabah.

1980 : Lee, D.T.C. studied satellite imageries of the west coast of Sabah in 1980.

1981 : Hoppe P., Weber H.S. and Yan A. as part of the Malaysian-German Mineral Exploration Project, all the stream sediment samples collected by the UNDP survey were reanalysed for Cu, Pb, Zn, Ni, Co and results were evaluated in 1981.

1981-82 : Hoppe, P. studied photogeology (1:50,000, 1:25,000 and Landsat imageries) of the Ranau-Kinabalu area between 1981 and 1982 as part of the Malaysian-German Mineral Exploration Project.

1983 : H.D. Tjia studied the Quaternary tectonics of Sabah and Sarawak (including the Ranau-Kinabalu area) in 1983.

PART II A,a(BAMBANGAN) AREA

Chapter 1 Geology and Mineralization

1-1 Geology

The A area is composed of late Cretaceous to early Miocene geosynclinal sediments (Trusmudi & Crocker Formations), peridotite which is supposed to have intruded after Cretaceous then tectonically emplaced in the sediments in early Miocene, and adamellitic rock which intruded in later Miocene. Quaternary Pinosuk Gravels covers all of them unconformably.

The wide distribution of Pinosuk Gravels extending from the central to the southern portion obscures the details of geology and geological structures. Judging from the point of geology of surrounding area, Trusmudi and Crocker Formations and peridotite have a trend to strike in a NW-SW system, dipping 30–45° southward. Adamellites consist of the adamellite (Kinabalu Mountains batholith), adamellite porphyry, microdiorite and granodiorite porphyry. The adamellite porphyry is characterized by large phenocrysts of K-feldspar. There are three principal fault systems in the area, i.e. N-S NE-SW and E-W systems.

The Bambang valley is along a fault line where dykes of adamellite porphyry and microdiorite have been intruded.

1-2 Mineralization

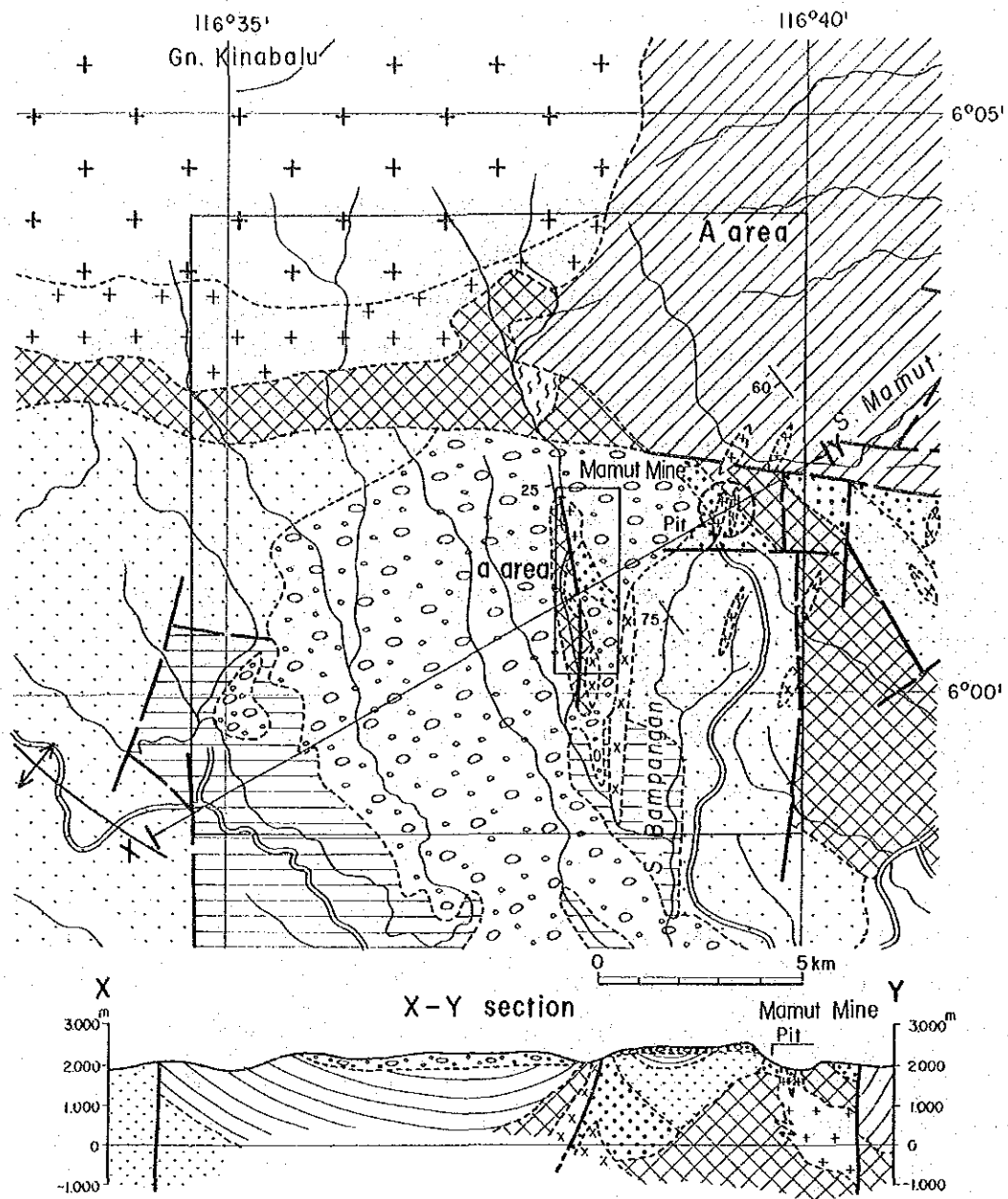
Mineralized zones in this area are known as the Mamut Mine and Bambang outcrops.

According to an old record, Bambang outcrops are located 20 m below the present road going to water intake for the Mine, occurring in brecciated adamellite porphyry and sandstone. The ore minerals are chalcopyrite, pyrrhotite, sphalerite and magnetite, and the highest grade in some part shows 10% of Copper content.

In 1970, Overseas Mineral Resources Development Co., Ltd. (OMRD) carried out a drilling work to investigate 40 m below the outcrop, however no fruitful result was obtained. At present, no outcrop can be found in the same landslide area. Above the present road, there is a small outcrop bearing malachite-pyrite dissemination in the same landslide area of adamellite porphyry, locating 100 m east-northeast from the old outcrop. The both outcrop seems to be the same along the extension of each others.

At the western bank of the Bambang Creek, about 800 m upstream from the water intake, a weak mineralized zone with malachite stain is exposed in an adamellite porphyry dyke.

The UNDP Survey (1963–1965) and OMRD (1970) detected geochemical copper anomalies, ranging from 480 to 960 ppm, in the middle course of Bambang Creek and in the upper and middle courses of Masilau Creek. In addition, on the eastern slope of the Bambang Creek,



LEGEND

- | | | | |
|---|--|---|---|
| <ul style="list-style-type: none"> Alluvial deposits Pinak Gravel Crocker Formation Trusmi Formation (unknown) Crystalline Basement | <ul style="list-style-type: none"> Boulders and gravels Sandstone, siltstone and mudstone Sandstone, mudstone and spilite and its pyroclastics Sandstone, mudstone and spilite and its pyroclastics Undifferentiated sedimentary and metamorphic rocks Schist and gneiss | <p>Igneous Rock</p> <ul style="list-style-type: none"> Microdiorite and Micro quartz diorite Adamellite porphyry Adamellite Serpentinized peridotite | <ul style="list-style-type: none"> Fault (certain) Fault (inferred) Strike and dip Anticline Geological profile line Area Survey area |
|---|--|---|---|

Fig. 7 Geological Map of "A" Area

it has been disclosed that the strong copper anomalies ranging from 1,000 to 3,000 ppm are distributed near the old outcrop and they extend into the Pinosuk Gravels area.

The Malaysian and West Germany joint survey team (1981) reconfirmed the occurrences of high copper anomalies over 3.0 km long at the same place in the Bambang Creek, showing the highest copper value of 1,790 ppm, and presumed that this area has the high potential for a large-scaled mineralization underlying the Pinosuk Gravels.

In order to further check the above-mentioned geochemical anomalies, OMRD conducted IP and SP surveys over the Mamute-Bambang area excluding the Pinosuk Gravels area. As a result, a narrow IP anomalous zone with a NE-SW trend was only detected on the eastern bank of Nasapan Creek.

However, it is well known that the high IP anomalies detected exactly on the Mamut deposits extend to NW-SE direction and tend to turn toward west in the further northern part.

As mentioned above, the Bambang area has been drawn attention as having a high potential for mineral explorations by the following reasons;

- (1) High geochemical copper anomalies have been obtained.
 - (2) Geology and structural system are quite similar to those of the Mamute area.
 - (3) Exploitation of deposits seems to be easier because of close vicinity to the Mamut Mine.
- With regard to these points, geophysical survey (CSAMT, IP and SIP methods) and drilling work were conducted in Phase I to explore the downward extension of the known outcrops and the potential horizon for ore deposit hidden underneath the Pinosuk Gravels.

Chapter 2 Geophysical Survey

2-1 CSAMT Survey

2-1-1 Objectives and Method of Survey

(1) Objectives

The geophysical technique CSAMT (Controlled Source Audio Magneto-Telluric) was first selected in order to correlate the geological structure of the zone under study with the subsurface electrical resistivity structure at depths. It will permit the selection of the most promising potential areas for the porphyry copper type deposit and will clarify the cause of the low resistivity of the zone.

(2) Method of Survey

i) The Conception of the Method

The geophysical prospection that makes uses of electromagnetic (EM) signals in the audio frequency range (10 Hz to 20 MHz) is known as Audio-frequency Magneto-Telluric (AMT) method. These signals come mainly from the activity of the electrical discharges of the atmosphere. Unfortunately, these methods have a great dispersion in the data, because of the variable location and the low levels of the thunderstorm which produce the signal. To overcome this problems, it has been devised a technique which utilizes instead an artificially induced current (electric dipole) as a controlled source. This is the reason why the technique is called : Controlled Source Audio Magneto-Telluric (CSAMT).

The CSAMT method has been used in mineral exploration for 10 years with significant success in the search for buried conductors. The system has shown a good lateral resolution and a good penetration.

A basic field setup is indicated in the Fig. 9. As it can be seen, the current is sent from the transmitter to a fixed dipole which ends in a certain number of steel stakes set on the ground. The measurements are taken at some distance, as far as practical, from the transmitter dipole, so that the EM waves traveling through the earth, behave as plane waves at the arrival in the receiver. For practical purposes, the depth of penetration can be related to the skin depth since it is a function of the resistivity of the underground surveyed area and of the frequency of the EM waves transmitted. The depth of penetration of the fields into the ground is directly related to the resistivity of the rock and inversely to the frequency applied. In a uniform earth, electric field (E) and magnetic field (H) decrease exponentially with depth. For this reason, this method uses the skin depth, being defined as the depth at which the EM fields fall to $1/e$ of their values at the surface. The skin depth is given by the following relation:

$$\delta = 503\sqrt{\rho/f}$$

where δ = skin depth in m.

ρ = earth resistivity in ohm-m.

f = frequency in Hz.

The effective depth d, can then be determined by the relation:

$$d = \delta/\sqrt{2} \approx 356\sqrt{\rho/f} \text{ (m)}$$

In this equation the frequency appears because the magnitudes of the induced currents depend on the time variation of the magnetic fields.

In the Fig. 8, it is shown a 3-D example of some CSAMT results over a massive sulphide orebody having a strong resistivity contrast.

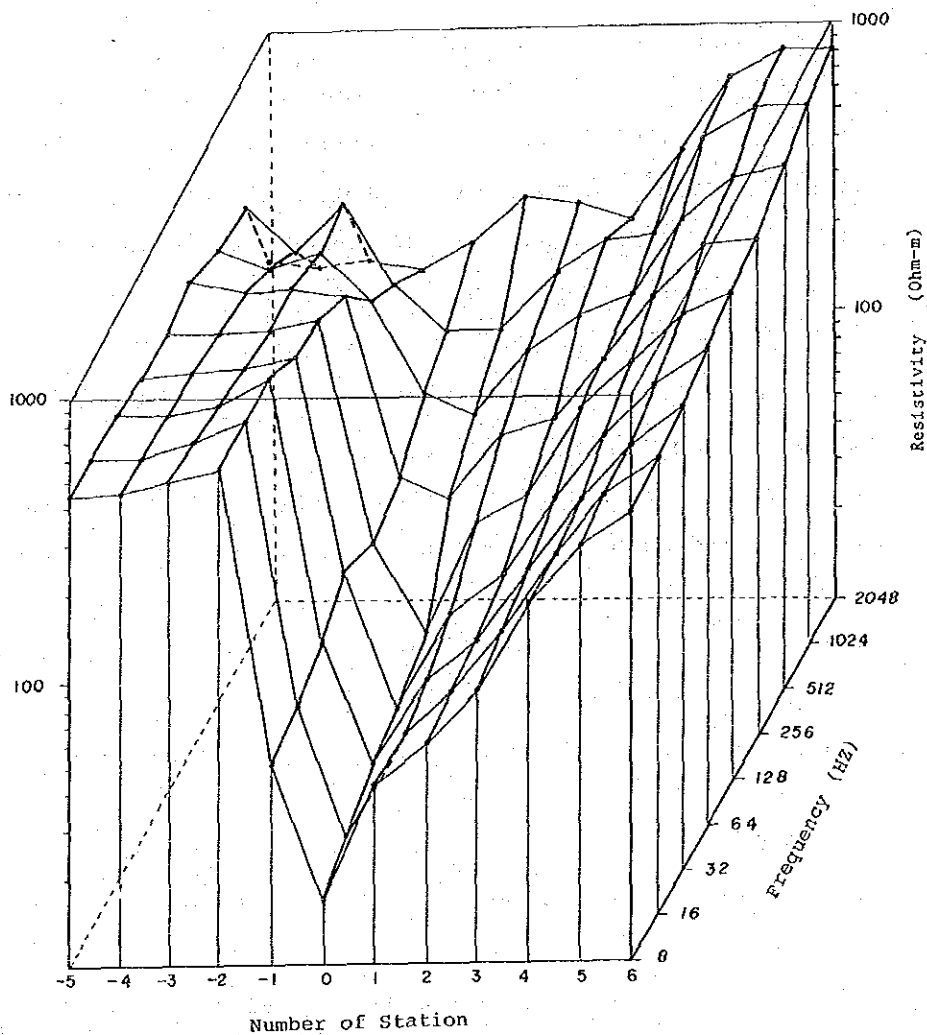


Fig. 8 CSAMT 3-D Display over a Massive Sulfide Orebody

ii) Instrumentation

To apply properly this technique, it is necessary to measure very weak magnetic fields by using a high sensitivity coil detector and to measure at the same time, extremely weak voltages generated in the ground.

The survey was carried out using an equipment manufactured by Zonge Engineering and Research Organization, U.S.A. The following table lists the parts utilized.

Unities	Component	Serial
1	Transmitter	GGT-25
1	Transmitter Controler	XMT-12
1	Motor Generator	AMG-20
1	Voltage Regulator	VR-1
2	Receiver	GDP-12/2GB
2	Cassette-Printer	CAP-12
2	Magnetic Field Antenna	ANT/2
1	Oscilloscope	Tektroniks 212
6	Porous Pot Electrodes	
100-120	Electrodes	

iii) Field Procedure

The dipole transmitter used an electrode separation of about 2.0 km. The transmitter controller permit to change the frequency in a discretized way in the audible range. In this survey, the transmitter sent currents at 10 different frequencies : 4, 8, 16, 32, 64, 128, 256, 512, 1,024 and 2,048 Hz. In each of the two electrode positions, from 50 to 60 electrodes were wired together and set to the transmitter by using an isolated wire.

The potential electrodes used consisted of 2 porous pots connected to ground in a parallel direction to the transmitter dipole for maximum electric field pickup and spaced about 50 m between them. For every frequency, it is measured the horizontal electric field, E_x , in the polar direction and the horizontal magnetic field, H_y , in the normal direction to the dipole. The electric field is determined by measuring the potential difference between the ends of the receiver dipole and the magnetic field by means of a high sensitive coil antenna centered on the dipole and moved about 10 m away from the receiver operator to minimize noise. The signals coming from the 2 EM fields, in sinchronization with the transmitter output, are fed to the receiver, which immediately stacks, accumulates and averages the data. The apparent resistivity is then

calculated according to the relation:

$$\rho = \frac{1}{2\pi f \mu} \frac{|E_x|^2}{|H_y|^2}$$

In practical units, where E is given in mv/km and H is in gammas, the magnitude is given by

$$\rho = \frac{1}{5f} \frac{|E_x|^2}{|H_y|^2}$$

The data so obtained are then printed and stored in a cassette printer made for that purpose in the field survey area, as E and H-field magnitudes and phase, resistivity, and relative phase between the two fields. The following indicates an example of the data stored in the cassette.

ST	: Station Number	
FREQ	: Frequency Code	*****0017
Gains	: Gain in the Receiver	ST 0192 FR006 4 HZ CSANT
Filter	: Notch Filter (01 = on)	GAINS 13 13 FILTER 00 STKS 0277
STACKS	: Stacking Times	A-SP050. COIL 1 GAIN01 CRNT 05.0
A-SP	: a-Spacing	ME +.1171113E-4 PE +.7863354E-1
Coil	: Coil Channel	MH +.1874738E-4 PH -.4316468E+0
Gain	: Gain of the coil	E +.2342221E-6 H +.2331752E-4
ME	: Measured Potential (v)	RHO +.5845901E+1 PD +.5182901E+0
PE	: E Phase (rad)	CI +.8848883E+0SEN +.8888888E+0
MH	: Magnitude of H (v)	*****0018
PH	: E Phase (rad)	ST 0192 FR006 4 HZ CSANT
E	: E-Field (v/km)	GAINS 13 13 FILTER 00 STKS 0265
H	: H-Field (mv/gamma)	A-SP050. COIL 1 GAIN01 CRNT 05.0
RHO	: Resistivity (ohm-m)	ME +.1873335E-4 PE -.1149625E+0
PD	: Phase Difference (PE-PH)	MH +.1679788E-4 PH -.4248708E+0
CK	: Coil Factor	E +.2147867E-6 H +.2889178E-4
		RHO +.5288935E+1 PD +.3891886E+0
		CI +.8848883E+0SEN +.8888888E+0

In this method, the stations should be located within a zone delimited by a 60° circular sector as indicated in the Fig. 9. Since the interpretation is based on a plane-wave source approximation for half space, the stations to be measured should be away from the transmitter source within a distance no closer than 3 times the skin depth.

Table 4 shows the details of the survey amounts and specifications.

Table 3 Specifications and Survey Amount for CSAMT Survey in "A" Area

Number of stations	204
Station interval	400–500 m
Electrode separation	Tx1 1550 m Tx2 1650 m
Area covered	100 Sq·Km

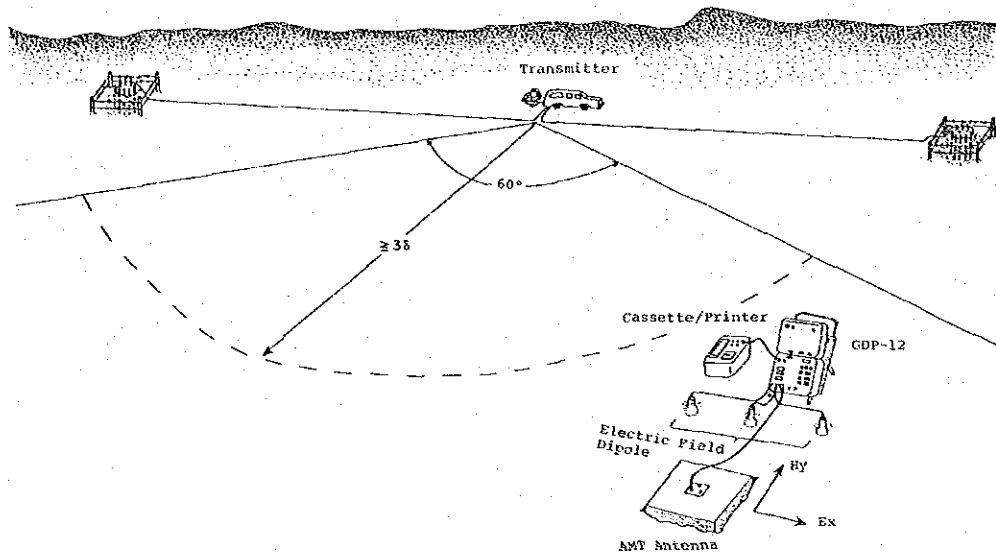


Fig. 9 Logistics of CSAMT Survey

2-1-2 Data Analysis

The data obtained from the field survey give the magnitude and phase of the electric and magnetic fields in every station and for every frequency. These data is automatically entered to the Data Processor (GDP-12), which computes the apparent resistivity, according to the equation given in the last section. It also computes the phase difference between the two fields. These data are obtained for every frequency in each receiver station.

The apparent resistivity obtained by the above process for every station, is then plotted as a function of the frequency in a log-log scale. The method of data analysis is based on the comparison of the sounding curves obtained in the field with theoretical curves for any combination of layer thickness and resistivity. This approach is followed by an inversion modelling analysis proposed by F. Bostick to make a multiple horizontal layering analysis in every station. In this process the apparent resistivity is calculated according to the equation:

$$\rho_a = -i \cdot \frac{Z^2}{\omega\mu}$$

where Z = wave impedance,

ω = angular frequency,

μ = permeability.

For a two-layer case, Z is given by:

$$Z = \frac{i\omega}{r_1} \coth(r_1 h_1 + \coth^{-1} \frac{r_1}{r_2})$$

where $r_1 = \left(\frac{i\omega\mu}{\rho_1}\right)^{1/2}$, $r_2 = \left(\frac{i\omega\mu}{\rho_2}\right)^{1/2}$,

h_1 = thickness of the first layer

ρ_1 = resistivity of the first layer

ρ_2 = resistivity of the second layer.

Combining both of these equations, results

$$\rho = -\frac{i\omega\mu}{r_1} \coth^2(r_1 h_1 + \coth^{-1} \frac{r_1}{r_2})$$

for n layers, the following equation can be applied:

$$Z = \frac{i\omega\mu}{r_1} \coth \left[r_1 h_1 + \coth^{-1} \left\{ \frac{r_1}{r_2} \coth \left(r_2 h_2 + \coth^{-1} \left[\frac{r_2}{r_3} \dots \dots \coth^{-1} \left\{ \frac{r_{n-2}}{r_{n-1}} \coth \left(r_{n-1} h_{n-1} + \coth^{-1} \frac{r_{n-1}}{r_n} \right) \dots \dots \right\} \right) \right\} \right]$$

where,

$$\rho_a = -i \frac{Z^2}{\omega\mu},$$

$$\mu = 4\pi \times 10^{-7} \text{ H/m}$$

$$\omega = 2\pi F,$$

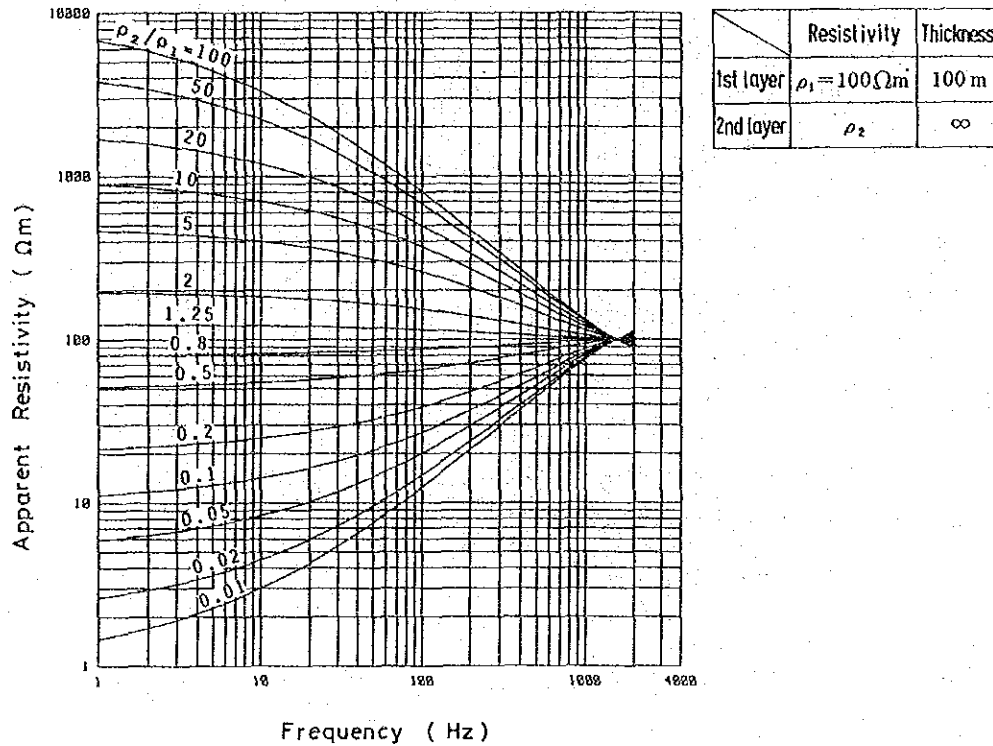
$$f \text{ in Hz}$$

$$r_n = \sqrt{\frac{i\omega\mu}{\rho_n}},$$

$$\rho_n \text{ in } \Omega\text{m}$$

$$h_n \text{ in m}$$

Two-layer Model Curve



2-1-3 Results of Survey

The apparent resistivities sections and plan maps obtained as a result of the data analysis, have given the following results:

(1) Apparent Resistivity Plan Maps

The apparent resistivities measured in the 10 frequencies are mapped for every frequency. Among them, the 5 frequencies of 2,048, 1,024, 512, 256 and 128 Hz were selected and shown in the Figs. 10-14 and maps 4-13.

In general, the resistivity distributions detected at the higher frequency range, show almost the same pattern as that shown at the lower frequency range. On the other hand, the resistivity change in this area shows a complex distribution with a strong resistivity contrast, with the exception of the central part near Kundasang.

(i) Resistivities higher than 100ohm-m are partly seen to the north, east and west of the area, surrounding the low resistivity zone of the central area. The high resistivity zones are splitted by faults into several blocks, indicating a complex geological structure as apparently seen near the Mamut mine.

(ii) A high resistivity of more than 100ohm-m in the north and west of the area is considered to be due to peridotite, while the one in the east near the south of Pit Site is considered to be due to sandstones and mudstones; distribution seems to correlate with the geology of the area.

This high resistivity is extended to the depths, showing the same pattern in the frequency range of 1,024–64 Hz. According to this geophysical technique, if an average resistivity of this resistivity body is 300ohm-m, then the skin depths becomes about 770 m at 128 Hz. Hence, this resistive body extends to the depths of 800 m from the surface, resulting more compact at depths.

(iii) A strong contrast in resistivity is seen near Mamut mine. A resistivity of less than 100ohm-m expands in the E-W direction, along which a high resistivity of more than 100ohm-m, related to the mineralization, is seen both in the west and the south. At 1,024 Hz, the resistivities at Nos. 167 and 60 near the Pit Site resulted more than 150ohm-m, however, it changes to less than 100ohm-m at 128 Hz. This low resistivity zone shows an E-W trending distribution, continuously extended to the west of the Pit, presenting a resistivity of less than 100ohm-m at the depths of 100 to 200 m.

Furthermore, this resistivity zone in the small area "a" extends to the low resistivity zone of the Kundasan Formation, forming in such way, a big scale fan shape-like with a low resistivity zone of less than 100ohm-m. In this zone, three promising low resistivity zones are detected. They are named as A-1, A-2 and A-3 and described as follows:

A-1 Resistivity Zone

To the west of Pit Site, the low resistive zone of elliptical shape coincide with the airborne magnetic anomaly previously detected. This low resistivity zone has a dominant resistivity distribution of 40–50ohm-m and includes a zone of a resistivity of less than 30ohm-m, which may reflect the resistivity of the fracture zone. This zone tends to increase its resistivity toward depths in the frequency range lower than 512 Hz, reflecting a change of the resistivities of the Pinosuk formation near the surface and that of the lower formation.

Judging from the fact that the thickness of the Pinosuk formation is around 50 m, then the low resistivity of 40–50ohm-m at lower depths are considered to be due to mineralization and alteration.

A-2 Resistivity Zone

In the "a" area, the low resistivity continues to the west of the A-1 zone, stretching to the E-W direction in the middle of the survey area. The IP survey carried out before in the "a" area showed no anomaly at all to the depth of 200 m.

In the "a" area, there are a big scale fault along the Bambang Creek and small scale faults parallel to it. The low resistivity of this area must be due either to ground water along this faults or to clay minerals filling the faults. From the no IP anomaly mentioned in the last paragraph, it can be inferred that no mineralized zone can exist in this area.

A-3 Resistivity Zone

This anomaly detected at the contact of a high resistivity zone, is considered to be due to the fault structure as A-2 and may be due to argillization in the resistive rock.

(iv) A low resistivity of 50–100ohm-m widely seen in the west of the Bambang Creek is divided into two by the low resistivity extending from “a” area and distributing over Kundasang. Here the resistivity distribution becomes monotonous, but showing two kinds of two-layered structures; the first one has a 50–70ohm-m for the upper layer with about 100 m thickness and 70–80ohm-m for the second layer. This structure is seen around Nos. 149, 128 and 109. The second one has a 100–200ohm-m for the upper layer. This is seen near the junction of the Bambang and Nasapang Creeks.

Consequently, if the resistivity of Pinosuk formation is 50–70ohm-m, the depth will be 100–150 m, increasing thickness gradually towards south.

(v) In the southwest of the area, as if splitted into several blocks by faults, resistivity of more than 100ohm-m are independently seen.

(2) Apparent Resistivity Sections

Apparent resistivities detected at each station are plotted in several apparent resistivity sections. To assist in the finding of the promising zones, four of these sections are shown on Figs. 15–18.

Section A

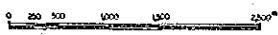
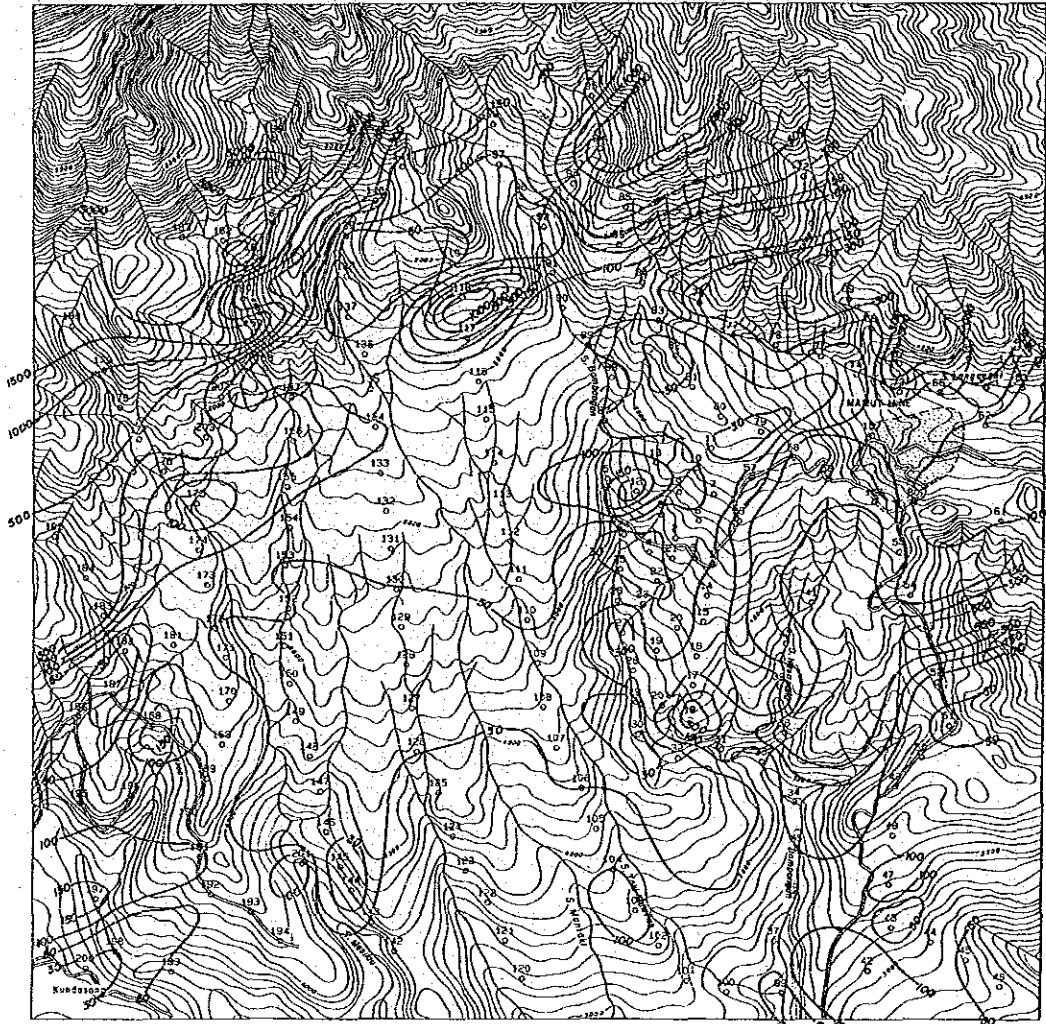
This section is along the N-S line and cutting the A-3 low resistivity zone. In this section and near No. 158, it is observed a resistivity boundary which may correspond to a fault. A high resistivity zone is found to the north of No. 158. However, a low resistivity zone is widely seen to the south of No. 158. The high resistivity correspond to peridotite which, judging from the resistivity change, must be compact at depth.

In the southern area of No. 157, it is assumed to be a two layered structure. However, in the south of No. 151, the resistivity at shallow depth becomes very low while at the depths it becomes higher.

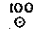
The low resistivity may be reflecting the spotted zones with abundant water and with a width of 1 km.

Near Nos. 158–154 the surface is resistive while at depths the formation becomes conductive. The reason for that must be due to the uplift of the second layer seen in the south of No. 151.

Faults are assumed near Nos. 160, 158 and 145. Other small scale faults are seen but not related to the objectives of this survey.



LEGEND

- 
Station and No.


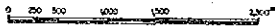
- 
Resistivity Contour

Fig. 10 Apparent Resistivity Plan Map in "A" Area (2048 Hz)



LEGEND

100
○ Station and No.


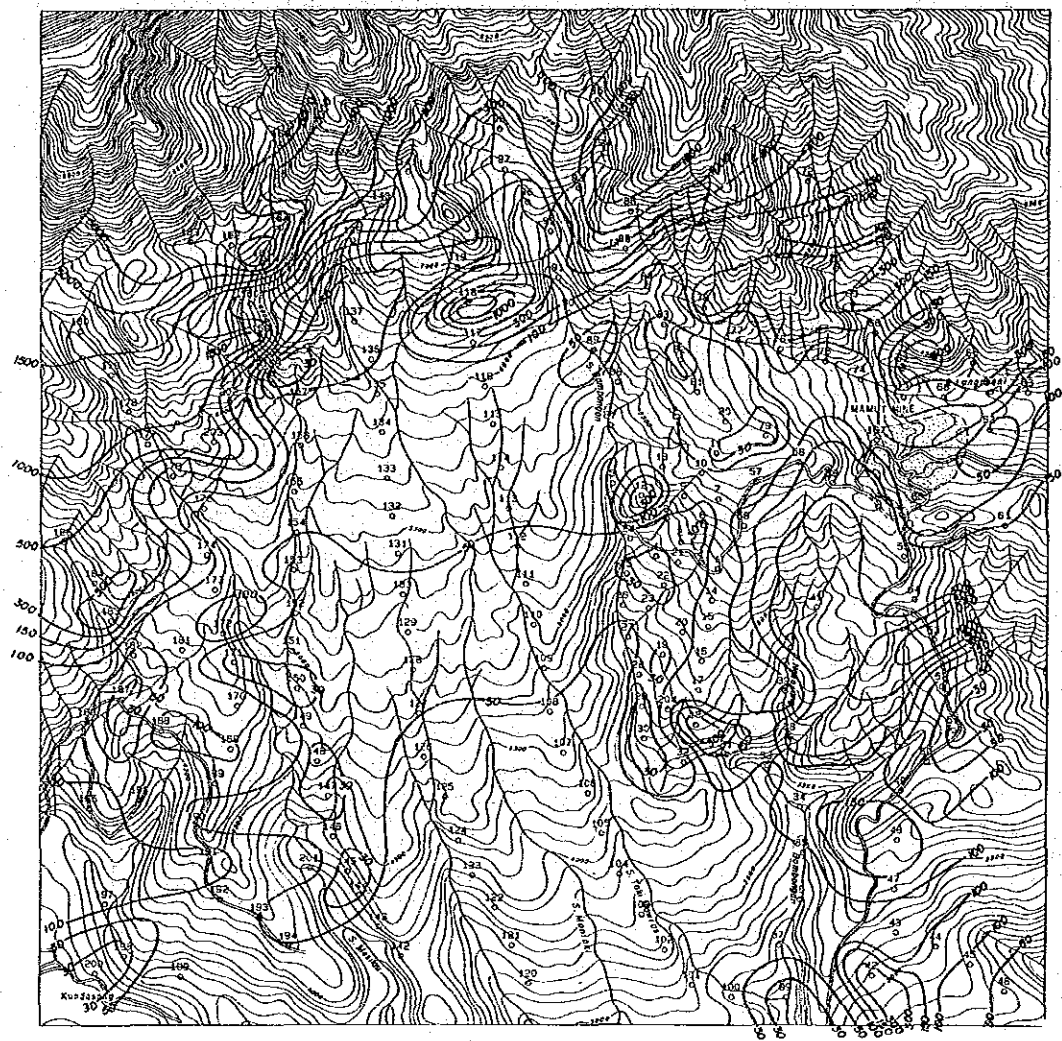
 Resistivity Contour

Fig. 11 Apparent Resistivity Plan Map in "A" Area (1024 Hz)



LEGEND

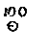

- 
Station and No.
- 
Resistivity Contour

Fig. 12 Apparent Resistivity Plan Map in "A" Area (512 Hz)



LEGEND

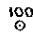

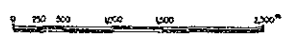
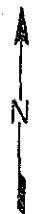
- 
Station and No.
- 
Resistivity Contour

Fig. 13 Apparent Resistivity Plan Map in "A" Area (256 Hz)



LEGEND

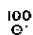

-  Station and No.
-  Resistivity Contour

Fig. 14 Apparent Resistivity Plan Map in "A" Area (128 Hz)

S

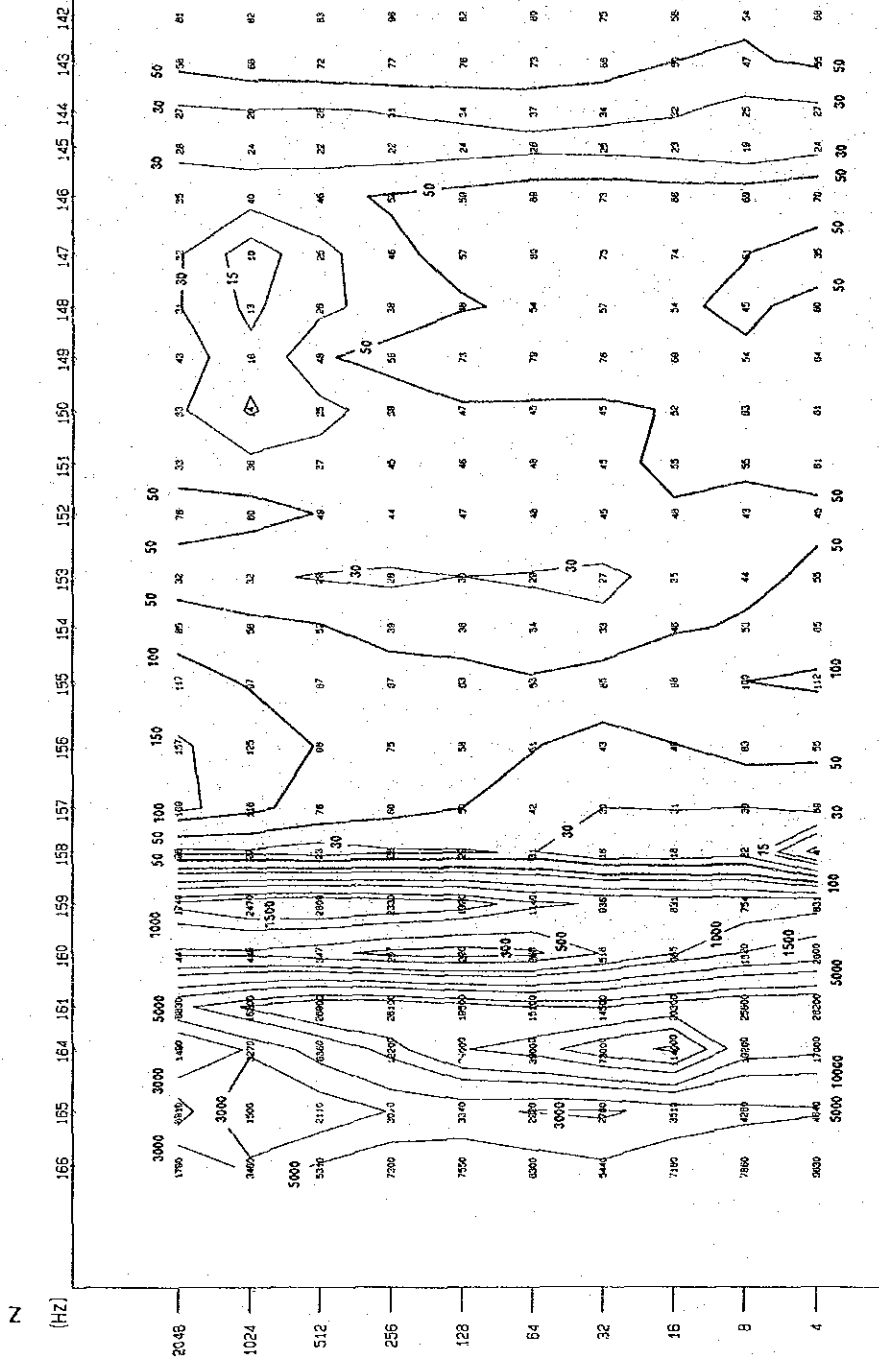


Fig. 15 Apparent Resistivity Section in "A" Area (Section A)

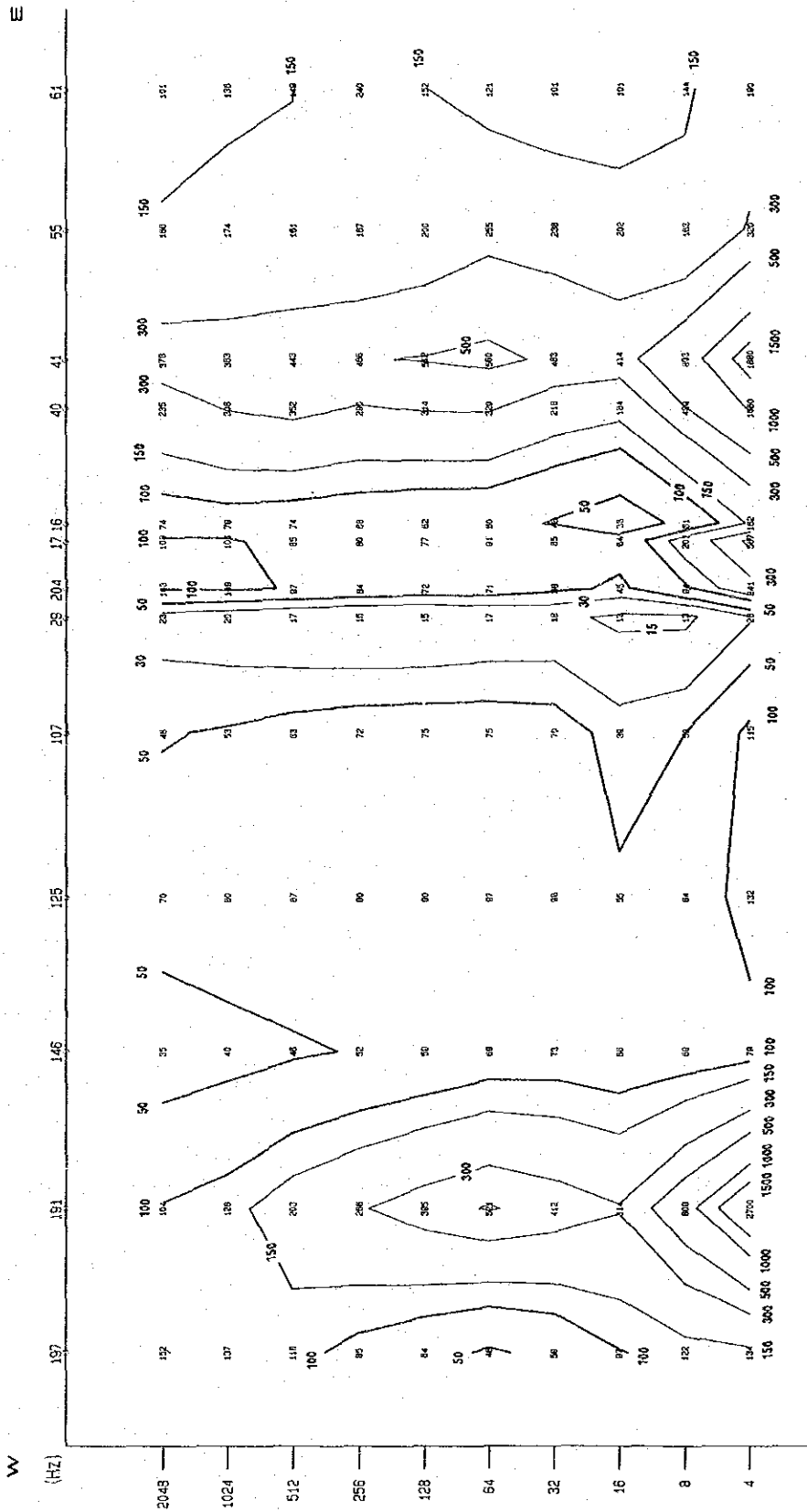


Fig. 16 Apparent Resistivity Section in "A" Area (Section B)

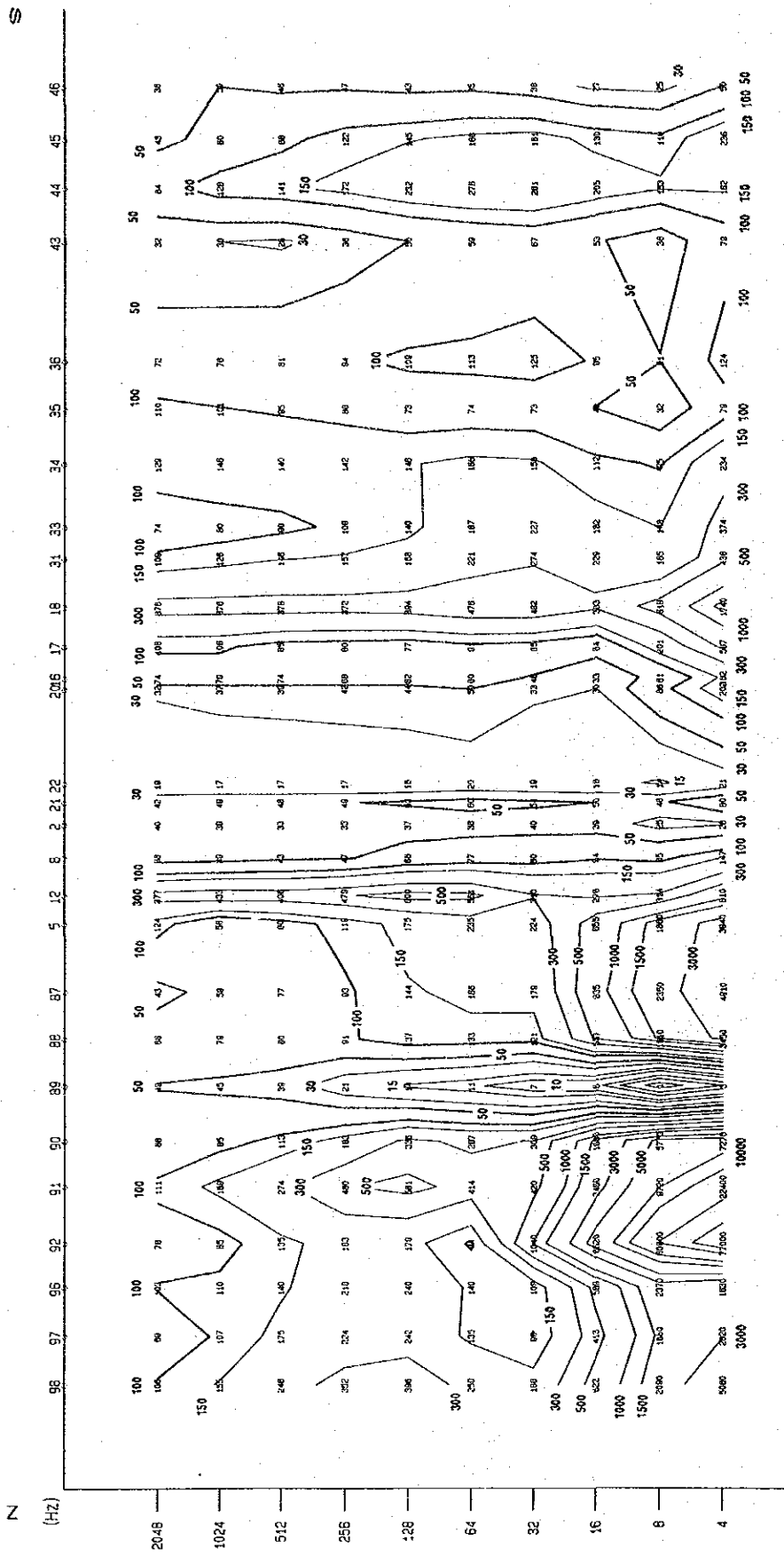


Fig. 17 Apparent Resistivity Section in "A" Area (Section C)

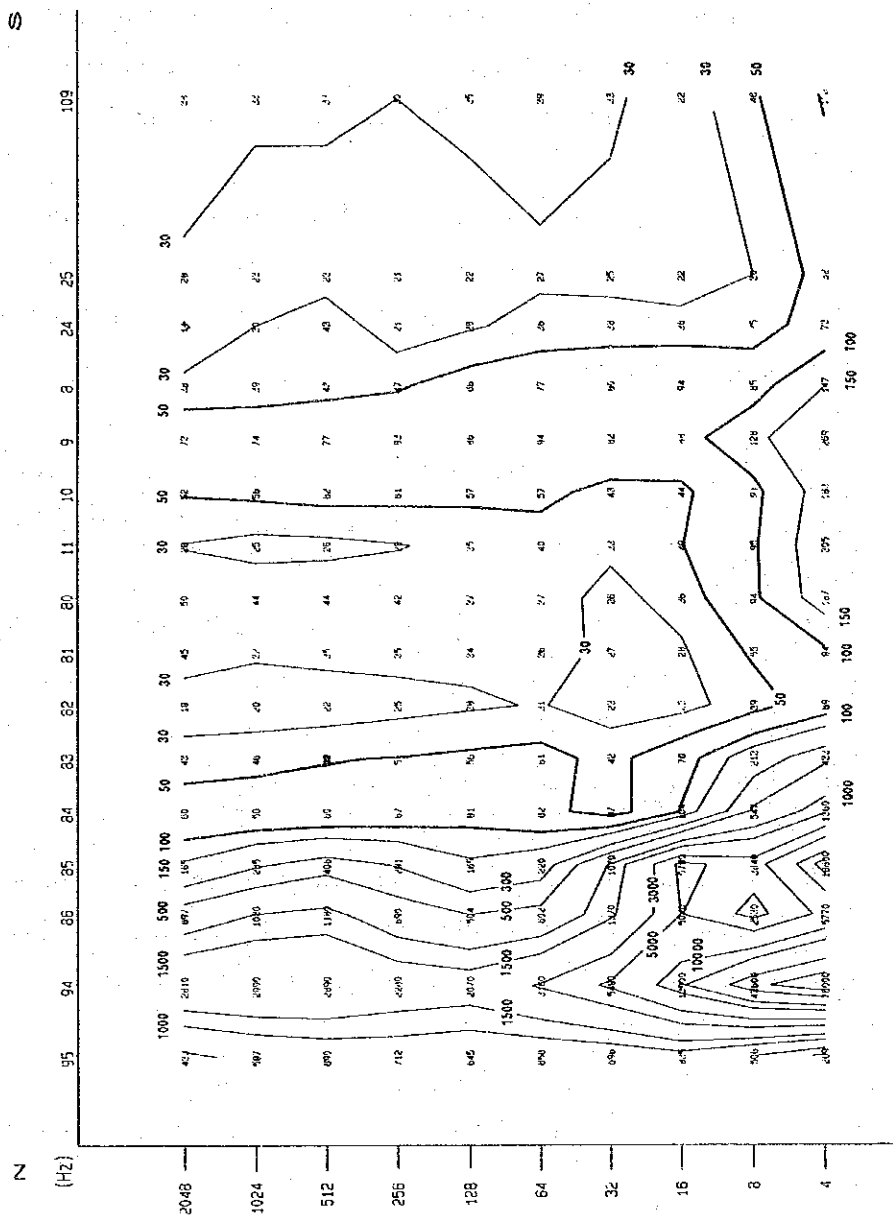


Fig. 18 Apparent Resistivity Section in "A" Area (Section D)

Section B

This is a NW-SE trending section passing through south of Pit Site and to the southern end of "a" area.

High resistivity zones are seen in both ends of this section. The high resistivity zone found in the west of Nos. 191–146 shows two layered structures with the first layer corresponding to Trusmadi Formation and the second to peridotite distributing in a dyke-shape at the lower part of Trusmadi Formation.

On the other hand, the high resistivity found at east of No. 40 may be due to thick and compact sandstone and mudstone.

Resistivities between 50 and 100ohm-m seen around Nos. 146–107 are considered to be caused by the thick Crocker Formation and its upper Pinosuk Formation.

Section C

This section, passing through "a" area along the Banbangan river, reflects the complex geological structure. An extremely low resistivity was detected between Nos. 96 and 87 in the low frequency range of less than 16 Hz.

The high resistivity detected in the whole section are divided by faults into several blocks. The high resistivity on the northern part of the section corresponds to the peridotite, while the southern part corresponds to resistivity rocks, such as mudstone. The low resistivity found at the shallow depths around Nos. 96–5 corresponds to Pinosuk Gravels.

Section D

This section penetrates the A-1 low resistivity zone. The high resistivity zone caused by peridotite is distributed to the north of No. 85. In the south of No. 85, resistivity of about 50 ohm-m widely distributed, where there is a lower Trusmadi Formation in which compact sandstone and mudstone may exist. The 50ohm-m resistivity zone must be due to argillization or mineralization in the lower part of the Trusmadi Formation.

Pinosuk Formation is widely distributed here but the resistivity contrast at shallow depth is so weak that the layer must be a thin or a strongly weathered layer.

(3) Resistivity Structural Map

Resistivities at 50 m, 150 m and 200 m below ground surface, derived from the results of 1–D inversion and 2–D model analysis, were plotted on plan maps and resistivity structural map at each depth was made as shown in Figs. 19–21 and Maps 14–16.

1) Resistivities of more than 100ohm-m are widely distributed at the northern, western and eastern portions of the area, and increase those distribution area with depth. And in the northern and western portions, resistivities are increased with depth so it is thought that

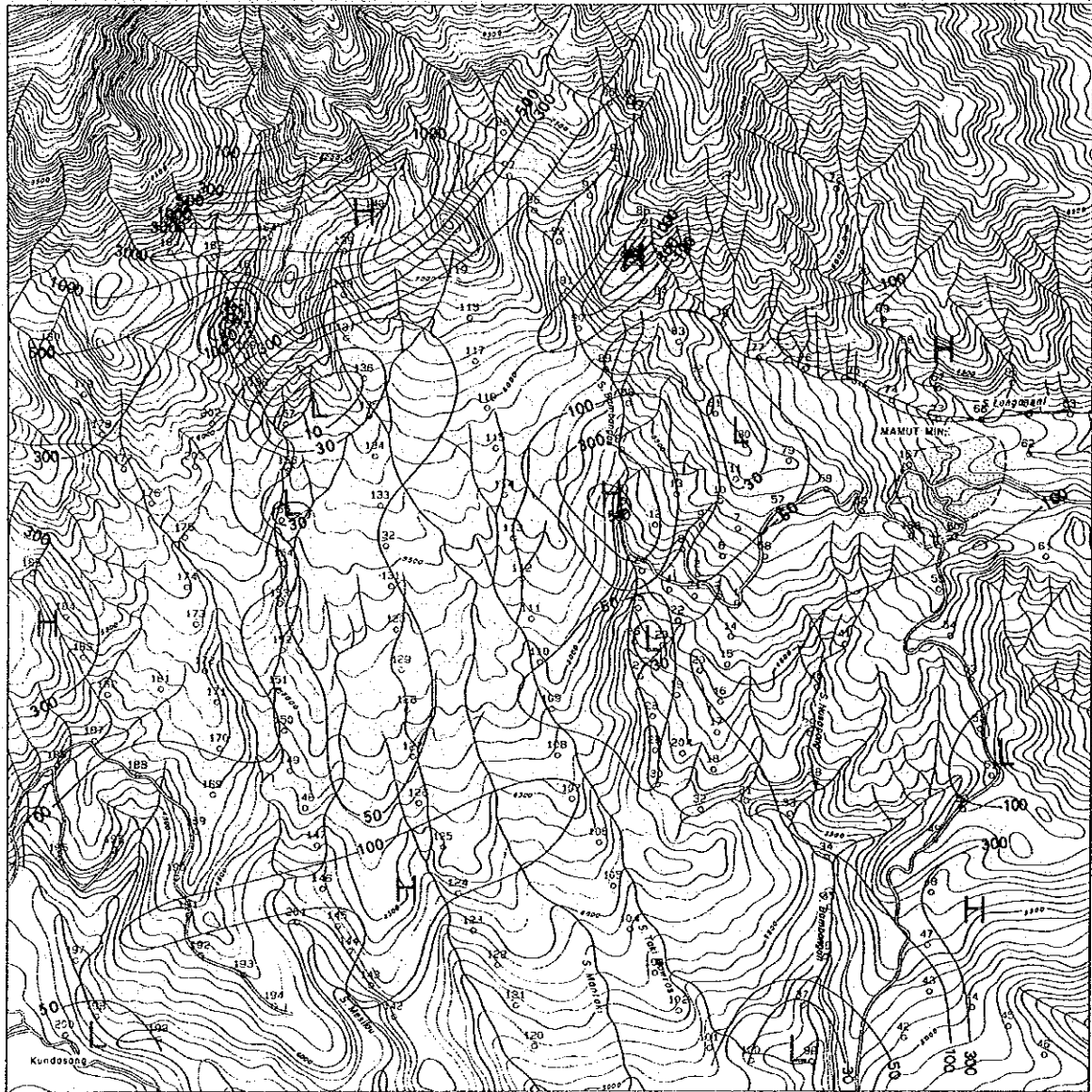


Fig. 19 Resistivity Structural Map in "A" Area (50m)

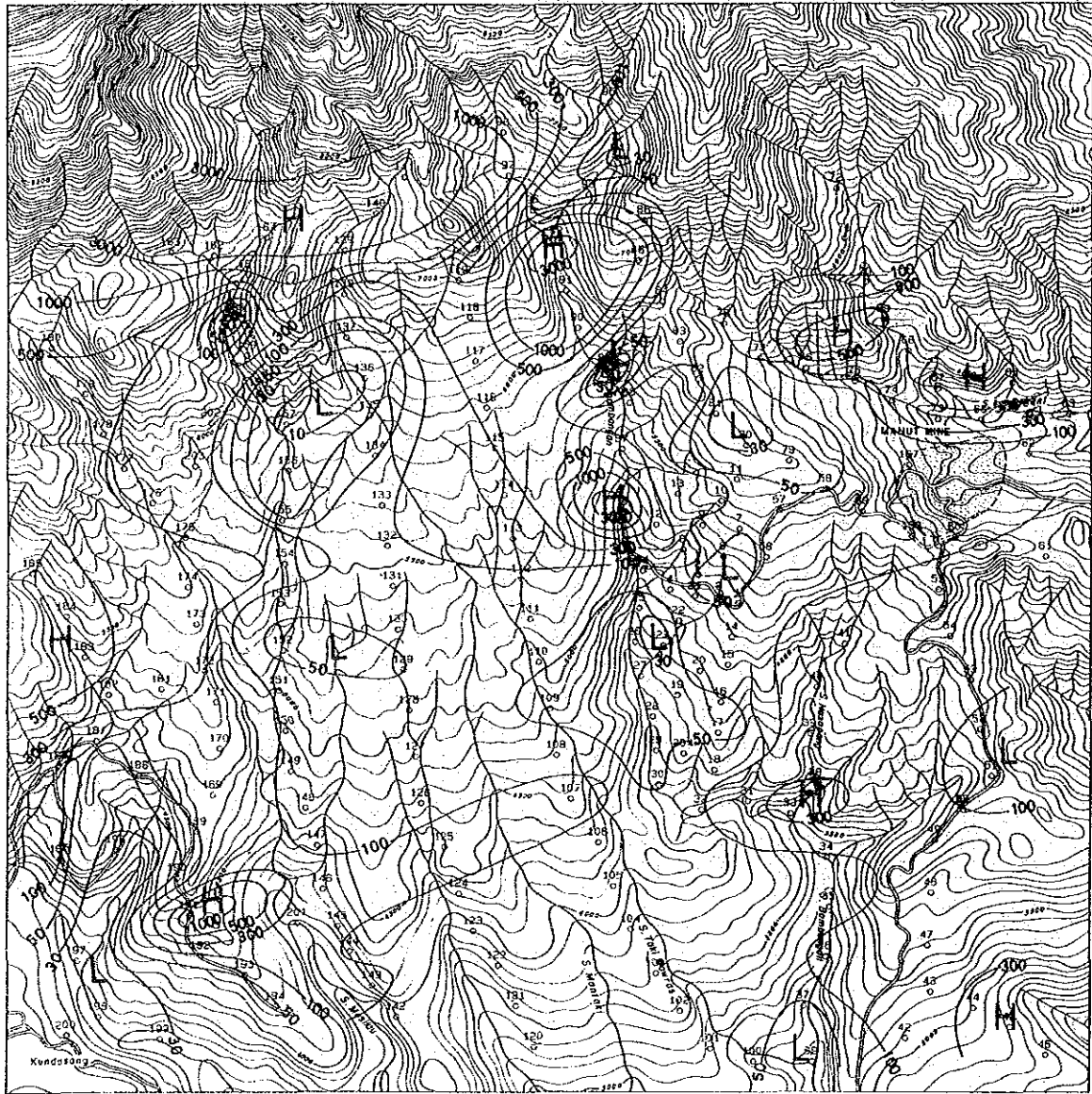


Fig. 20 Resistivity Structural Map in "A" Area (150m)

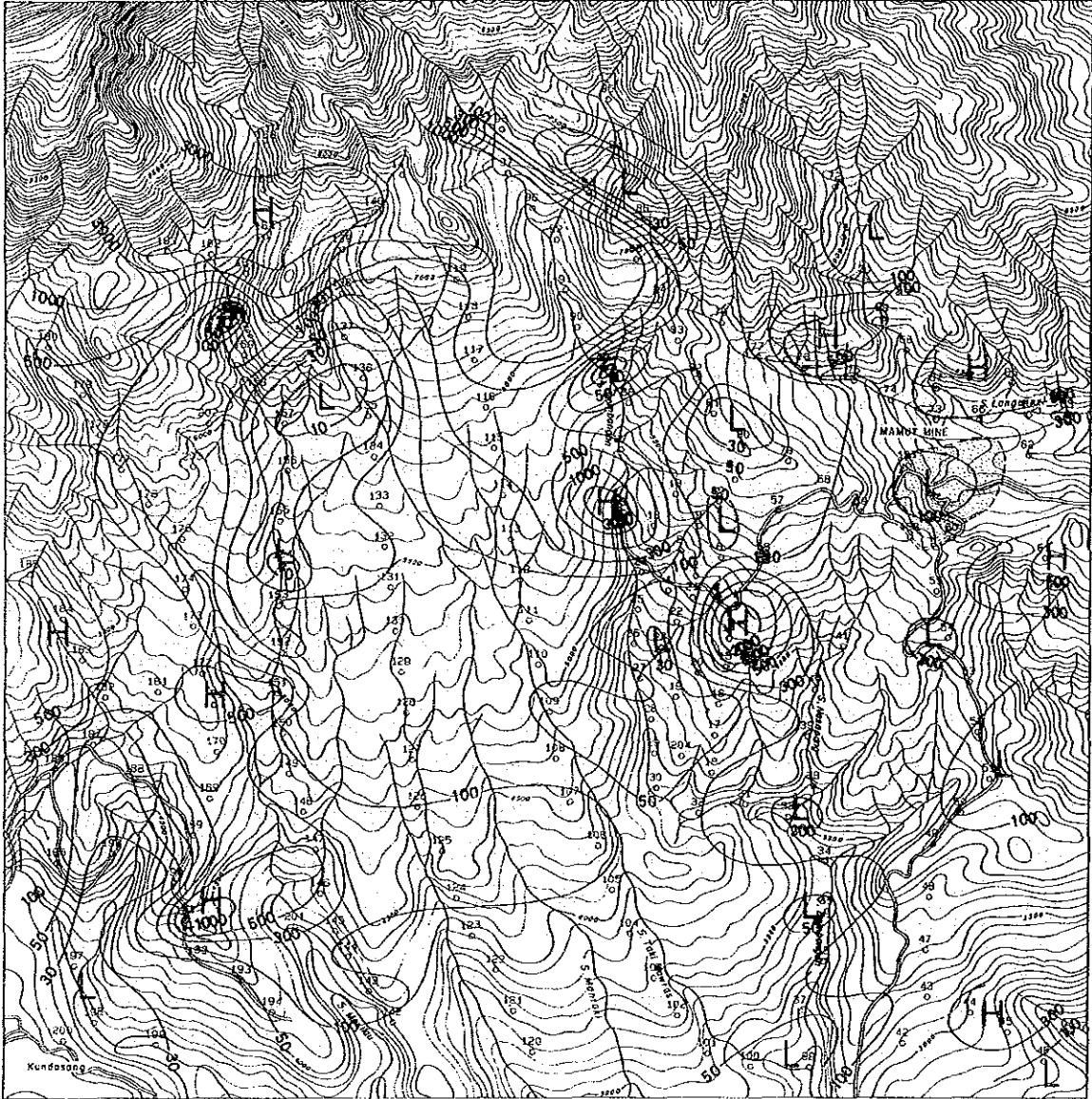


Fig. 21 Resistivity Structural Map in "A" Area (200m)

causative rocks may be more compact than those of ground surface.

Those at the northern and western portions, and eastern portion may reflect peridotite and sandstone/mudstone, respectively.

2) Low resistivities of less than 100ohm-m are surrounded by above-mentioned high resistivities, and are divided into several small blocks in depth, which may suggest that fault structures are developed in depths.

3) Three resistivity zones inferred using apparent resistivity maps are distributed as follows:

A-1 resistivity zone; At the shallower depth, it shows a broad distribution with extending in N-S direction, but in depths its distribution is limited only near No. 81. This zone may correspond to Pinosuk Formation at depth of shallower depth than 50 m, and to mineralization and/or argillization at depths. This zone is connected to A-2 resistivity zone at the southwestern corner.

A-2 Resistivity zone; This zone is divided into two zones, eastern and western zones, at all depths. The former, located in the "a" area, and the latter tend to be connected to A-1 and A-3 resistivity zones, respectively.

A-3 resistivity zone; Low resistivities of less than 10 ohm-m are distributed at each depth, and an area of resistivities of less than 30ohm-m increases with depth so it is connected to A-2 resistivity zone at depth of deeper than 150 m. This low zone may be caused by either fracture zones associated with NE-SW trending fault and small faults crossing it, or mineralization/argillization.

4) At the depth of shallower than 150 m, resistivities of more than 50ohm-m and less than 100ohm-m are predominantly distributed within the Pit Site of Mamut mine, and at the both sides, north and south, resistivities of more than 100ohm-m are found.

(4) Resistivity Section

Based on results of 1-D inverse analysis of each station, 2-D model analysis were made for four sections (A, B, C and D) and the results are shown in Fig. 22-25.

Section A

A four-layer structure is assumed at the central part (between Nos. 158 and 146) of the section.

First layer is of resistivity of less than 40ohm-m with a thickness of 50-60 m, and second layer is of resistivity of about 50ohm-m, which shows a little difference from that of first layer. The latter is of a thickness of 120 m at a fault inferred near No. 151, 150 m near No. 155, and 30 m between Nos. 155 and 158. As the Pinosuk Formation is distributed between Nos. 158 and 146, these first and second layers may be corresponded to this for-

mation.

Third layer of resistivity of more than 70ohm-m is the thickest, 650 m, between Nos. 153 and 146, and is about 30 m thick between Nos. 156 and 154, where a high resistivity body of more than 100ohm-m is assumed in depth. This third layer may correspond mainly to Crocker Formation which is mainly consisted of sandstone and is a lower formation of the Pinosuk Formation.

On the other hand, a single layer structure suggesting the existence of a highly resistive rock is found on the north side of a fault inferred near No. 158. These highly resistive rocks of more than 100ohm-m may reflect peridotite.

Section B

Both sides of the section, west of No. 146 and east of No. 46, shows a single layer structure suggesting the existence of a highly resistive rock of more than 100ohm-m from ground surface.

A two- and/or three-layer structure is found between Nos. 146 and 16. First layer of a resistivity of about 50ohm-m shows a thickness of 50–70 m between Nos. 146 and 147, and of 250 m near No. 16. Second layer of a resistivity of 70–90 ohm-m increases its thickness toward south, but can not be seen at the north of No. 29, where second layer is same as third layer being found between Nos. 146 and 107. Third layer of a resistivity of more than 100ohm-m is distributed thickly at the depth of more than 200m between Nos. 146 and 107.

As Pinosuk Formation is distributed between Nos. 146 and 16, first and second layers in this portion may correspond to this formation. And highly resistive layer and/or body of more than 100ohm-m may correspond to peridotite like the section A.

Faults and/or geotectonic lines are assumed at four locations, at No. 146, in depth between Nos. 146 and 125, between Nos. 107 and 29, at No. 17 and between Nos. 16 and 40.

Section C

A three layer structure is assumed at the whole section, and the lowest layer of low resistivity shows a dome-like structure in depths between Nos. 33 and 44.

At the north of No. 12, resistivity and thickness of first layer is of 100ohm-m and of 100 m, respectively. Second layer is a high resistivity one of more than 100ohm-m.

Between Nos. 12 and 20, resistivity of first layer is less than 50ohm-m. Second layer of a resistivity of 50–100ohm-m is the same as first layer at the north of No. 12, and also corresponds to first layer at the south of No. 31.

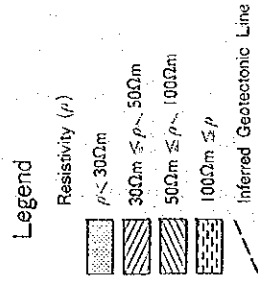
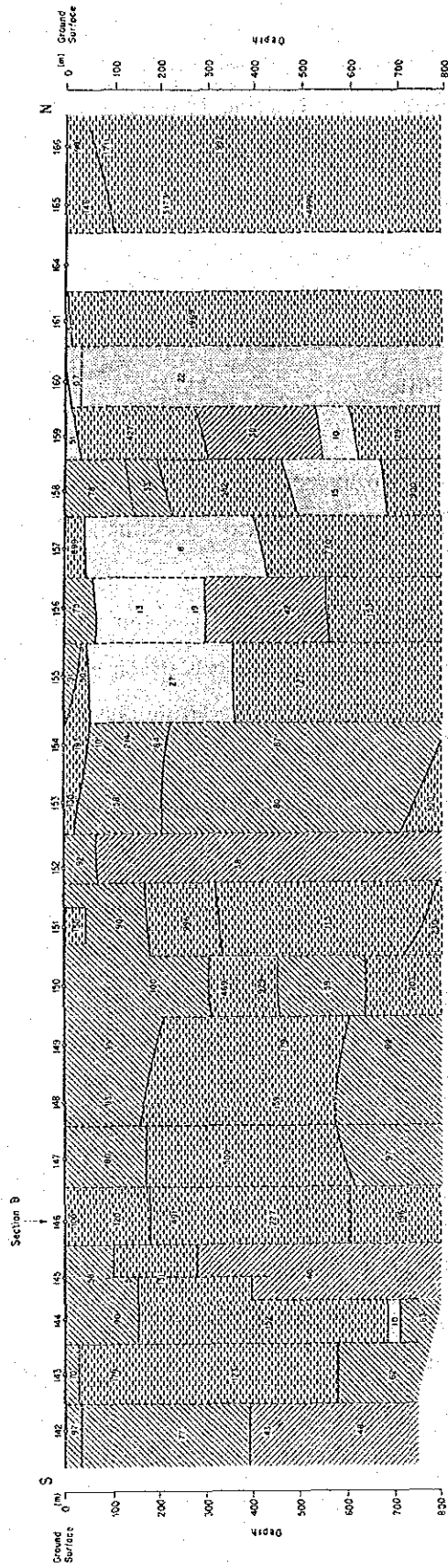
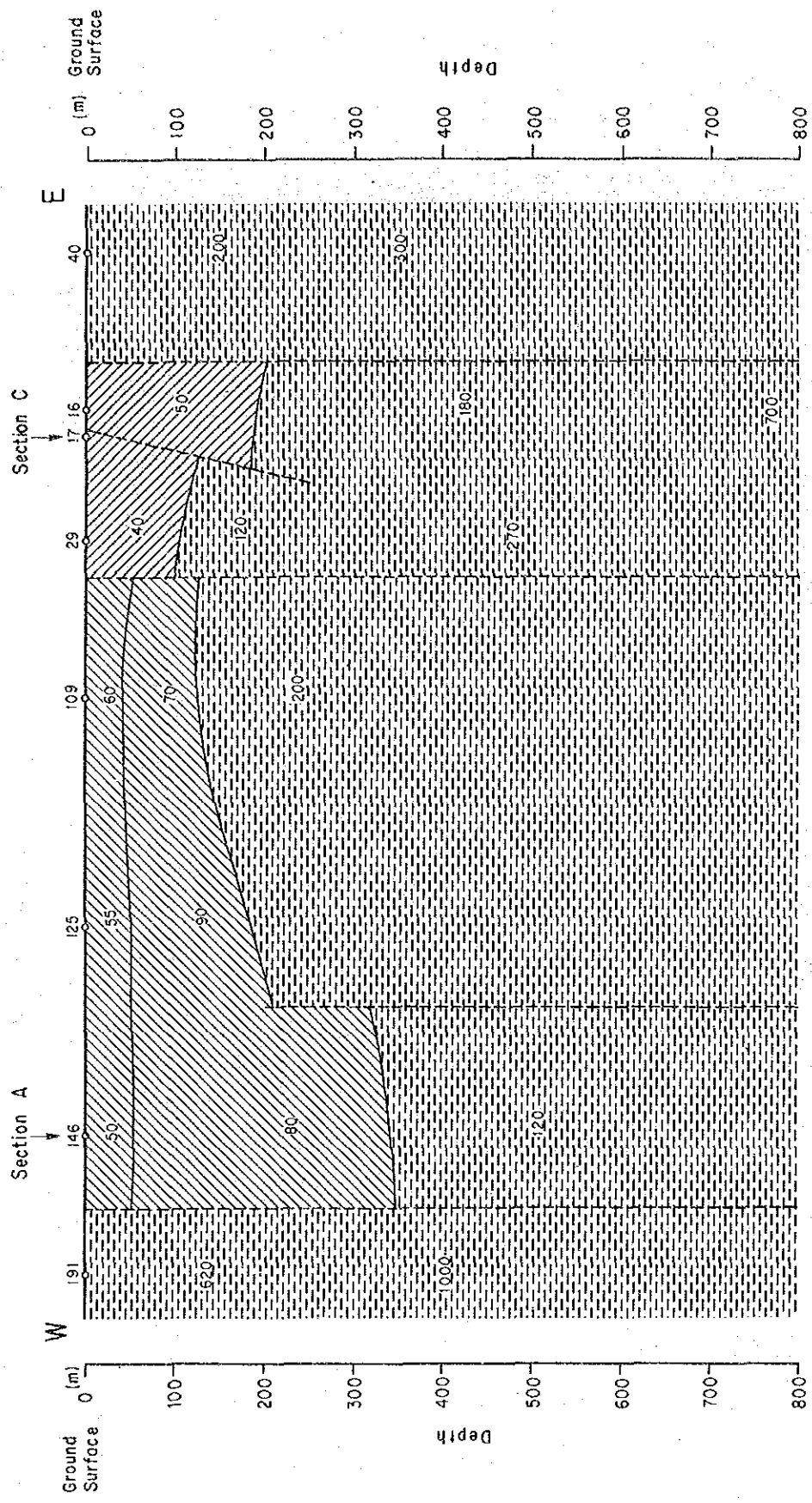


Fig. 22 Resistivity Section in "A" Area (Section A)



Legend

Resistivity (ρ)

- $\rho < 300 \Omega m$
- $300 \Omega m \leq \rho < 500 \Omega m$
- $500 \Omega m \leq \rho < 1000 \Omega m$
- $1000 \Omega m \leq \rho$

Inferred Geotectonic Line

Fig. 23 Resistivity Section in "A" Area (Section B)

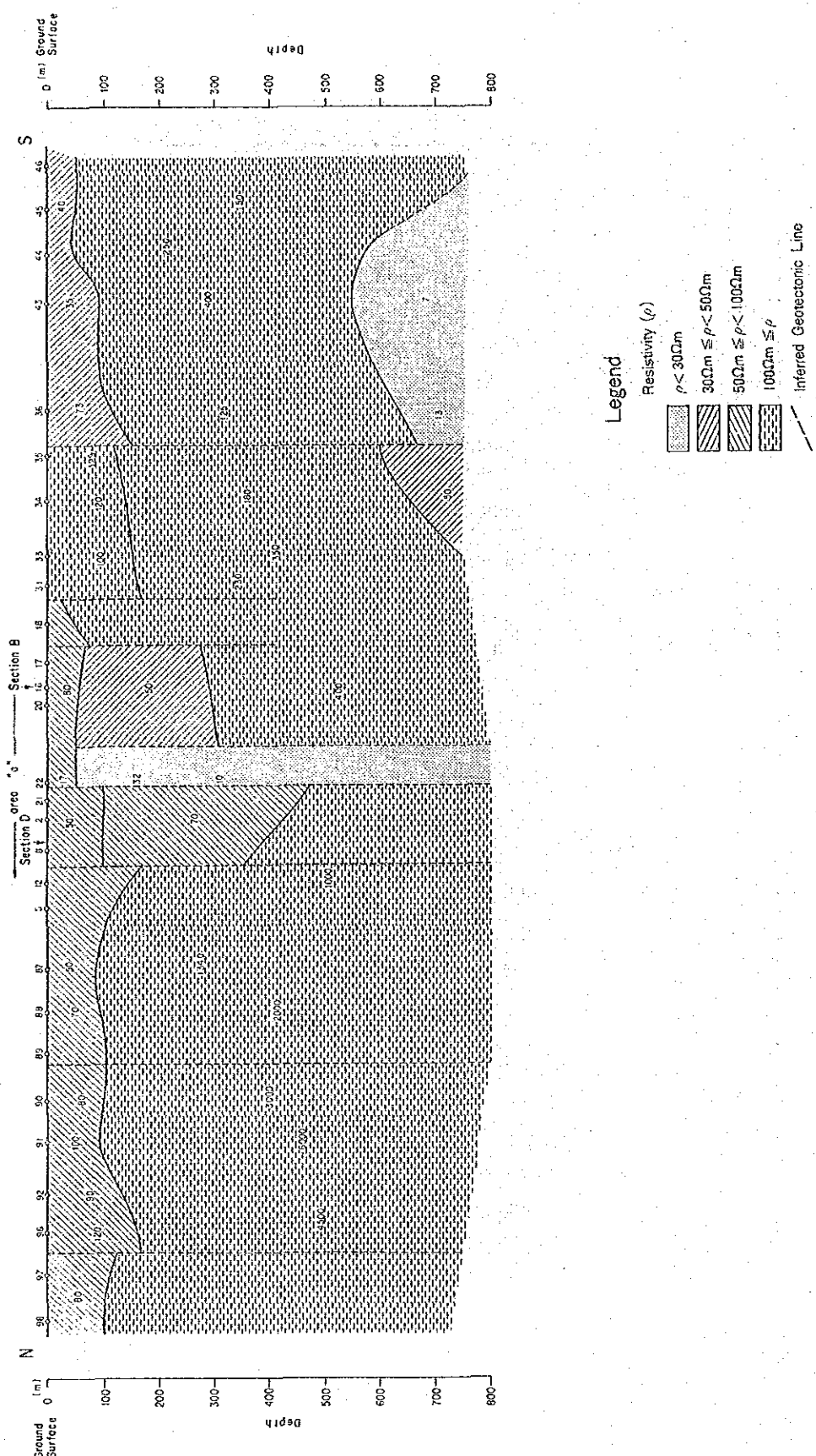


Fig. 24 Resistivity Section in "A" Area (Section C)